Spring 2022

Primary cilia display a non-uniform response to intracellular calcium release

Hannah R. Fisher
Western Washington University, fisherh3@wwu.edu

Primary cilia display a non-uniform response to intracellular calcium release

By

Hannah R. Fisher

Accepted in Partial Completion
of the Requirements for the Degree
Master of Science

ADVISORY COMMITTEE

Dr. Nick Galati, Chair

Dr. Jose Serrano-Moreno, Co-Chair

Dr. David Leaf

Dr. Jeff Young

GRADUATE SCHOOL

David L. Patrick, Dean

Master's Thesis

In presenting this thesis in partial fulfillment of the requirements for a master's degree at Western Washington University, I grant to Western Washington University the non-exclusive royalty-free right to archive, reproduce, distribute, and display the thesis in any and all forms, including electronic format, via any digital library mechanisms maintained by WWU.

I represent and warrant this is my original work and does not infringe or violate any rights of others. I warrant that I have obtained written permissions from the owner of any third party copyrighted material included in these files.

I acknowledge that I retain ownership rights to the copyright of this work, including but not limited to the right to use all or part of this work in future works, such as articles or books.

Library users are granted permission for individual, research and non-commercial reproduction of this work for educational purposes only. Any further digital posting of this document requires specific permission from the author.

Any copying or publication of this thesis for commercial purposes, or for financial gain, is not allowed without my written permission.

Hannah R. Fisher

May 31, 2022

Primary cilia display a non-uniform response to intracellular calcium release

A Thesis
Presented to
The Faculty of
Western Washington University

In Partial Fulfillment
Of the Requirements for the Degree
Master of Science

by
Hannah R. Fisher
May 31, 2022

Abstract

Cilia are microtubule-based organelles that project from the surface of individual cells. When cilia are formed, they are nucleated from centrioles that are known as basal bodies. Microtubules elongating from the basal body give rise to the axoneme of the cilium, which gives cilia their rod-like structure. The axoneme is surrounded by a specialized plasma membrane that is unique, but continuous with the plasma membrane that surrounds the rest of the cell. The ciliary membrane is enriched with ion channels and membrane bound proteins that are essential for cilia function. Interestingly, the cilium maintains a distinct environment from the rest of the cell, despite there being no membrane separation from the area within the cilium (i.e., ciliary compartment) and the rest of the cell. Cilia function includes generating hydrodynamic force for motility and participating in signal transduction that is necessary for sensation and animal development. Calcium ions (Ca^{2+}) are necessary for cilia to achieve these functions, yet questions remain as to how Ca^{2+} levels are maintained within cilia (i.e., ciliary Ca^{2+} levels). The current "outside-in" model suggests that Ca^{2+} channels fill cilia with Ca^{2+} from outside of the cell (i.e., extracellular) and that Ca^{2+} can diffuse freely between the ciliary compartment and inside of the cell (i.e., intracellular; Delling et al. 2016). However, the base of the cilium can be embedded within the Golgi apparatus (i.e., Golgi), which is a rich source of intracellular Ca^{2+}. Since the Golgi modulates Ca^{2+} levels at other cellular structures (Follit et al. 2006; Micaroni et al. 2012), this raises the question – does the Golgi impact ciliary Ca^{2+} levels from inside the cell? We first tested this by disrupting the structural integrity of the Golgi with Brefeldin A (BFA) and found that on average cilia from cells treated with BFA show higher Ca^{2+} than cells treated with the DMSO control. To further test the current "outside-in" model, histamine and thapsigargin were used to stimulate the release of Ca^{2+} from the Golgi and endoplasmic reticulum (i.e., ER), which

are both rich intracellular Ca^{2+} stores. Unexpectedly, Ca^{2+} released from the Golgi and ER did not freely diffuse into cilia, as predicted by the "outside-in" model. Rather, cilia displayed a non-uniform response to intracellular Ca^{2+} release, suggesting that free diffusion is not the underlying mechanism of Ca^{2+} transfer from intracellular Ca^{2+} stores into the ciliary compartment. Experiments involving mechanical stimuli and the Ca^{2+} channel blocker, lanthanum (III) chloride ($LaCl_3$) show that cilia display a more homogeneous response to extracellular Ca^{2+}. This work suggests that cilia display a differential response to Ca^{2+} dependent on whether Ca^{2+} is of intracellular or extracellular origin, consequently, expanding the current "outside-in" model of ciliary Ca^{2+} homeostasis. To continue testing this model in future studies, a custom cell line of NIH 3T3 fibroblast cells (Arl13b-GCaMP6-mCherry) was developed to permanently express the genetically encoded Ca^{2+} sensor used to quantity Ca^{2+} in cilia in this study.

Acknowledgements

I would like to acknowledge my thesis advisor, Dr. Nick Galati, and my committee members, Dr. David Leaf, Dr. Jose Serrano-Moreno, and Dr. Jeff Young for their guidance and support. I would also like to acknowledge the Western Washington University Biology Department for providing support and funding for my research through the Fraser Fellowship, Chair Funds, as well as a teaching assistantship. In addition to the Biology Department, I want to acknowledge the Office of Research and Sponsored programs for awarding me the RSP Fellowship. I would like to thank the members of the Galati lab, particularly, Josh McNamara. Josh's time and dedication to the cloning portion of this project was commendable and made the process of obtaining our cell line possible. His work on centrosome positioning and IFT20 localization also greatly contributed to this research. Finally, I'd like to express my gratitude towards the friends and family members that have encouraged me along the way. I'd like to especially thank my partner and my grandparents for their unwavering support.

Table of Contents

List of Tables and Figures

Introduction

Part I – Background on cilia and their relationship to calcium signaling

Cilia overview and significance

Cilia are microtubule-based organelles that project from the surface of individual cells. Cilla are evolutionarily conserved and found abundantly across species including protozoa, nematodes, and vertebrates (Mitchison et al., 2017). Cilia function includes generating hydrodynamic force for motility and participating in signal transduction that is necessary for sensation and animal development. When cilia are formed, they are nucleated from two centrioles that comprise what is known as the basal body (Dawe et al., 2007). Centrioles are cylindrical structures that are responsible for arranging microtubules. In Eukaryotic cells, centrioles are essential for guiding chromosomes during cell division. Cilia are formed by a process known as ciliogenesis in G1 or G0 of the cell cycle when centrioles dock at the cell membrane to form the basal body (Figure 1B; Ishikawa et al., 2011). Docking is achieved by the tethering of transition fibers to the plasma membrane (Szymanska and Johnson 2012). Microtubules elongating from the basal body give rise to the axoneme of the cilium, which gives cilia their rod-like structure. The growth of cilia requires the active transport of cilium-specific proteins and membrane proteins, which is achieved by the intraflagellar transport (IFT) system (Figure 5; Ishikawa et al., 2011). The axoneme is surrounded by a specialized plasma membrane that is unique, but continuous with the plasma membrane that surrounds the rest of the cell. The ciliary membrane is enriched with ion channels and membrane bound proteins that are essential for cilia function. Interestingly, the cilium maintains a distinct environment from the rest of the cell, despite there being no membrane separation from the area within the cilium (i.e., ciliary compartment) and the rest of the cell.

Cilia were first discovered in 1647 by Leeuwenhoek when numerous hair-like beating structures were visible through light microscopy. These structures were given the name cilia, Greek for "eyelash." The evolutionary origin of cilia can be traced back approximately 1 billion years (Carvalho-Santos et al., 2011; Mitchell et al., 2017; Sigg et al., 2017). Since their origin, cilia have evolved and filled niches across various species and domains of life. Currently, there are 187 established and 241 candidate cilia-associated genes in the human genome (Reiter et al. 2017). Mutations in any of these genes can disrupt cilia and cause devastating disorders known as ciliopathies, which can lead to a range of conditions such as infertility, retinal degeneration, polycystic kidney disease, and brain anomalies (Reiter et al., 2017; Hildebrandt et al., 2011). Expanding our understanding on how cilia function and interact within an intricate network of intracellular proteins and organelles will reveal insights into a deeply conserved biological process as well as illuminate basic processes that underlie human disease.

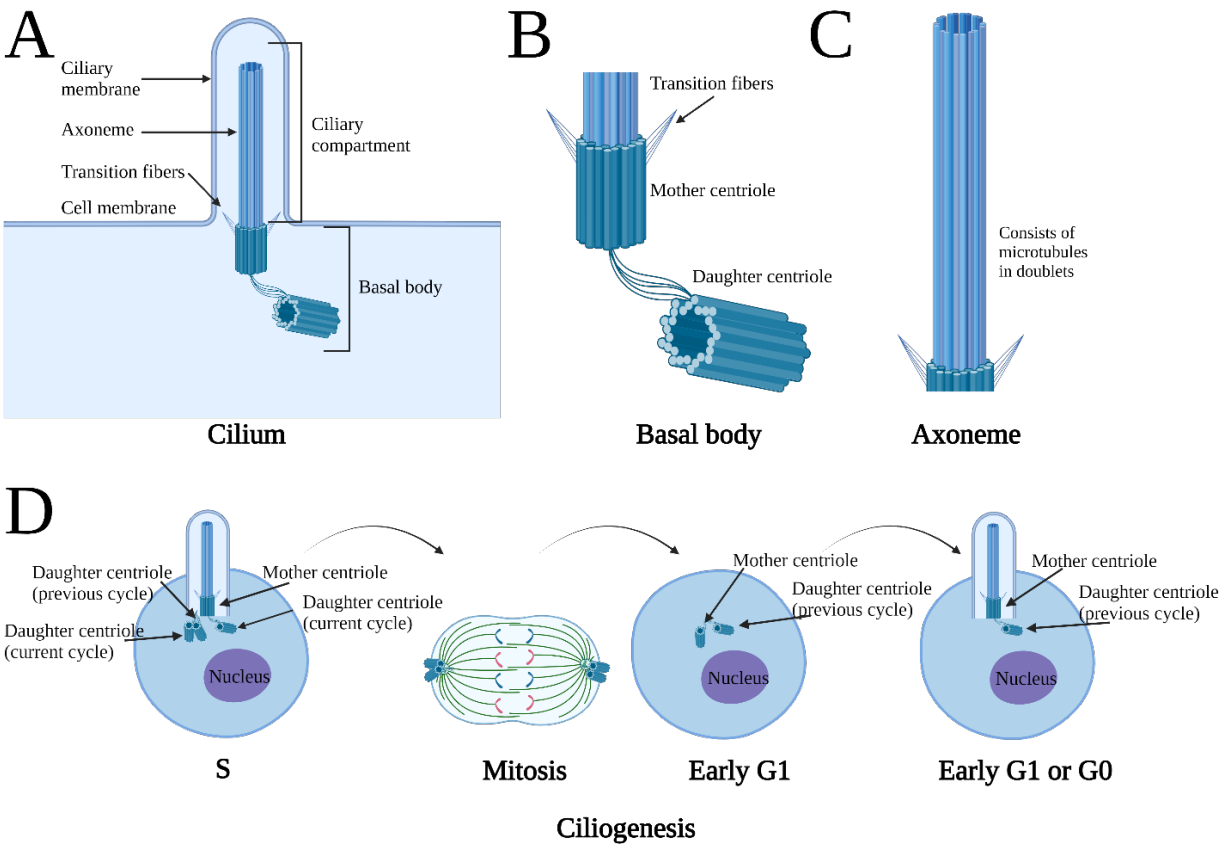

Figure 1. Cilia structure and formation
(A) Schematic of a cilium as a whole with key structures identified. **(B)** Zoomed in schematic of the mother and daughter centriole that comprise the basal body. Transition fibers are also identified, which aid in membrane docking. **(C)** Zoomed in schematic of the axoneme. The axoneme is comprised of sets of doublet microtubules that extend from the basal body. **(D)** An overview of the state of cilia at each point in the cell cycle. Cilia are formed in early G1 or G0.

Motile cilia and Ca^{2+} dependent functions

Functionally, cilia are divided into two categories, motile, and non-motile (i.e., primary cilia; Figure 2A). Although motile and primary cilia perform different biological functions, both motile and primary cilia rely on calcium ions (i.e., Ca^{2+}). Motile cilia are whip-like, and they generate hydrodynamic force by beating in a coordinated manner to move fluid. Motile cilia function is conserved among evolutionarily district organisms, serving many biological niches to that aid survival. Motile cilia display an increase in beat frequency in response to Ca^{2+} (Inaba, 2015). Single-cell protists such as *Tetrahymena* require an influx of ciliary Ca^{2+} to utilize motile cilia to push them through their aquatic environment (Doerner et al., 2015). In the fallopian tubes of mammals, motile cilia require an influx of Ca^{2+} to generate hydrodynamic force to propel the ovum from the ovary to the uterus (Ezzati et al., 2014).

Primary cilia and Ca^{2+} dependent functions

Primary cilia are stationary, and they receive chemical, mechanical, and optical signals (Reiter et al., 2017; Figure 2B). Primary cilia can extend beyond the cell surface or remain submerged in a membranous pit. Primary cilia participate in a variety of signaling pathways, one of which is the sonic hedgehog (Shh) signaling pathway, a pathway critical for cell differentiation, embryonic development, and tumorigenesis (Blum et al., 2015; Moore et al., 2016). Primary cilia are also responsible for vision, residing in light sensitive cells (i.e., photoreceptors) of the retina in both vertebrates and invertebrates (Morshedian et al., 2017; Nilsson, 2013). Similarly, olfactory cilia contain the odorant receptors that detect chemical signals during olfaction (Kleene et al., 2014).

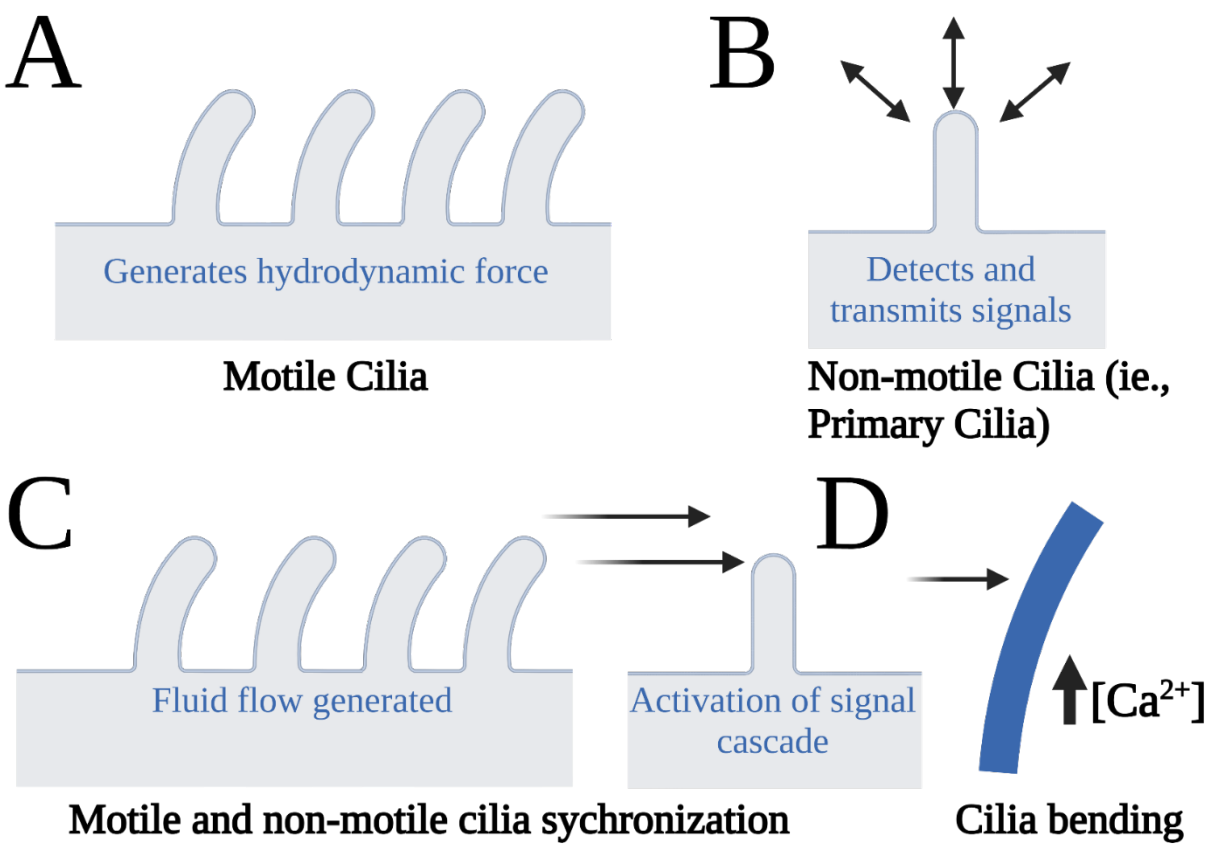

Figure 2. Motile and non-motile cilia structure and function
(A) Motile cilia showing the generation of hydrodynamic force through coordinated beating of each cilium. **(B)** Non-motile cilia detect extracellular cues and transmitting signals. **(C)** Motile cilia shown producing fluid flow through coordinated beating of cilia. This hydrodynamic force can be detected by non-motile cilia and result in signal transduction. **(D)** Non-motile cilium detecting fluid flow from extracellular environment. This bending can cause an increase in ciliary Ca^{2+} levels.

Coordination of motile and primary cilia and Ca^{2+} dependent functions

Despite differences in function, both motile and primary cilia rely on Ca^{2+} to execute many of their diverse roles. In some cases, the hydrodynamic force generated by motile cilia is sensed by primary cilia. An example of the role that Ca^{2+} plays in coordinating motile cilia and primary cilia occurs early in mammalian development when cilia work in conjunction to establish the L-R asymmetric body plan in mammals. To do so, motile cilia projecting from the ventral aspect of the embryonic node experience an influx of Ca^{2+} and rotate in a clockwise direction, generating a leftward fluid flow known as 'nodal flow.' Nodal flow has been proven necessary for biasing L-R asymmetry in the mouse embryo (Okada et al., 1999; Nonaka et al., 2002; Figure 2C). The unidirectional flow is sensed by primary cilia on crown cells at the periphery of the embryonic node (Yoshiba et al., 2012), which converts asymmetric Ca^{2+} transients in cilia and the cytoplasm of crown cells into asymmetric developmental cues that lead to asymmetric organ placement (Mizuno et al., 2020). When the Ca^{2+}-sequestering protein parvalbumin is overexpressed at cilia, asymmetric Ca^{2+} transients do not enter the cilium, which disrupts the process of generating L-R asymmetry (Mizuno et al., 2020). When L-R asymmetry is disrupted, it causes a deviation from an asymmetric body plan (i.e., *situs solitus*), a condition known as *situs inversus* occurs. Consequences of L-R asymmetry breakage influences organ placement and causes a wide range of birth defects and life-long genetic disorders (Grimes et al., 2017). In addition to diseases caused by the breaking of L-R asymmetry, cilia can have further impacts on human health.

There are currently 35 established diseases caused by mutations in cilia and cilia-associated proteins. Some of these ciliopathies can have devastating impacts such as retinal degeneration,

renal disease, cerebral anomalies, and infertility (Reiter et al., 2017; Figure 3). The list of emerging ciliopathies continues to grow as additional research is conducted to study cilia in both an unperturbed and altered state through techniques in cell biology, molecular biology, genetics, and biophysics. Due to the importance of Ca^{2+} in cilia biology and the intricate involvement of ciliary Ca^{2+} in development and human health, we seek to grow our understanding of how cilia utilize and contribute Ca^{2+} to and from the surrounding environment. While research on intracellular Ca^{2+}stores such as the ER and the Golgi apparatus (i.e., Golgi) is well-established, many questions remain as to how intracellular Ca^{2+} stores contribute to Ca^{2+} dependent signaling at cilia. Mizuno et al. 2020 showed that Ca^{2+} transients in the cilia and cytoplasm of crown cells of mouse embryos were detected and that IP3 pathway activation was essential for the generation of L-R asymmetry in cytoplasmic Ca^{2+} in crown cells. The activation of the inositol 1,4,5-triphosphate (IP3) pathway releases $Ca^{2+}$from the ER and Golgi, suggesting that intracellular Ca^{2+} stores are important in the generation of L-R asymmetry.

The role of Ca^{2+} in the cell

From the beginning of life, cells have required the ability to adapt to changes in their environment. For multicellular organisms to effectively control and modulate cellular conditions, there must be a level of coordination both within the cell and with the extracellular environment (Verkhratsky and Parpura, 2015). One way this coordination is achieved is by using chemical messengers which can include any compound capable of transmitting cellular messages such as hormones, neurotransmitters, and ions. Ca^{2+} is a critical secondary messenger that serves as a vital communicator of cellular information ranging from excitability, exocytosis, motility, apoptosis, and transcription (Carafoli and Krebs, 2016).

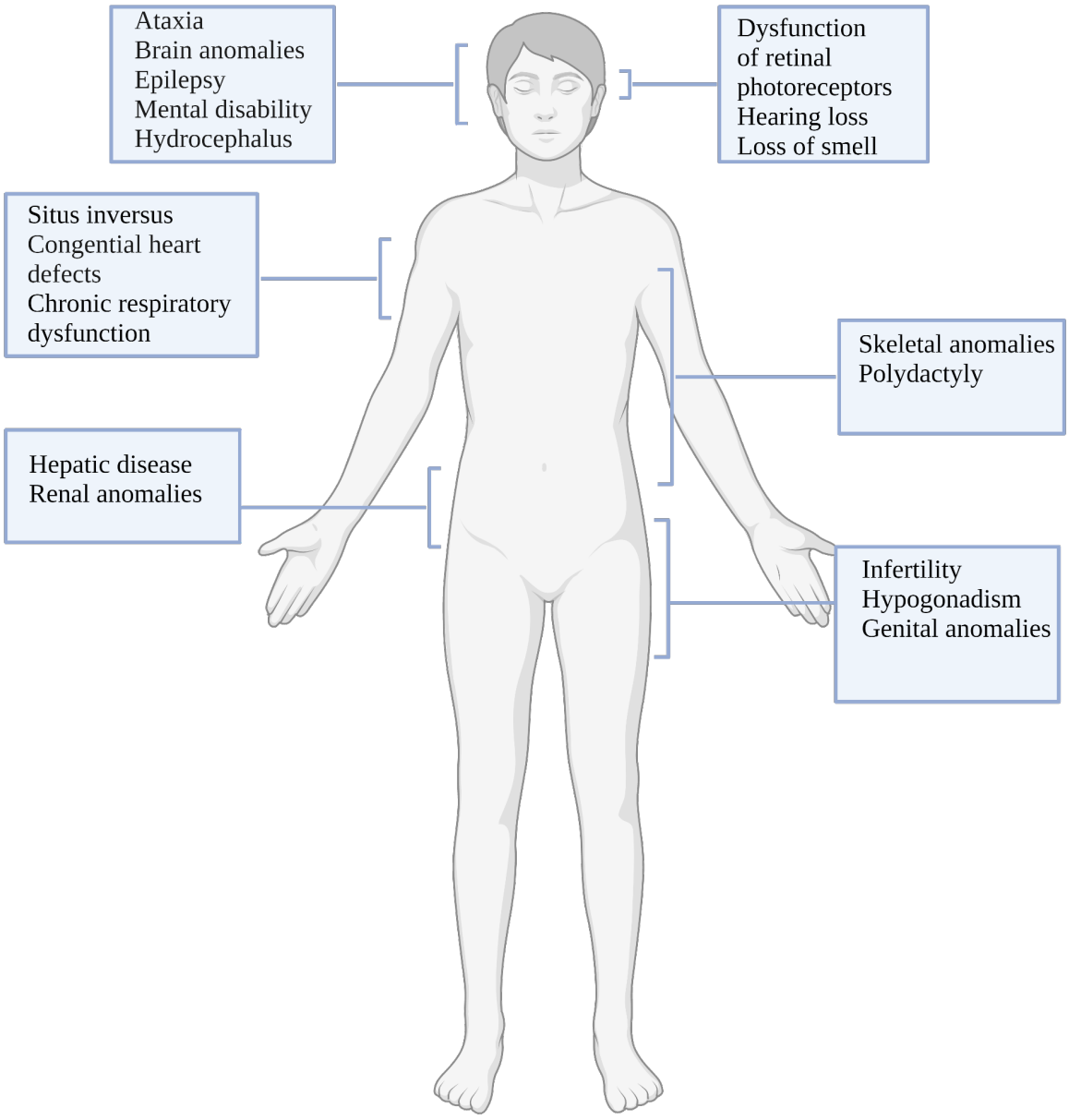

Figure 3. Cilia and human health implications
Examples of the possible implications of mutated cilia or cilia-associated proteins on the human body. These ciliopathies can cause a wide range of developmental disorders and diseases.

Cells evolved elaborate mechanisms to control intracellular Ca^{2+} levels (Marchadier et al., 2016). The mechanisms governing intracellular Ca^{2+} levels rely on a combination of proteins that bind Ca^{2+} (i.e., Ca^{2+}-binding proteins), ion channels/pumps, and internal structures that store Ca^{2+} (i.e., Ca^{2+} buffering organelles). Ca^{2+}-binding proteins have highly conserved protein domains that bind Ca^{2+}. Some Ca^{2+} binding proteins act as Ca^{2+} receptors, while others serve as Ca^{2+} storage proteins (Prins et al., 2011). Much of what we understand about the regulators of intracellular Ca^{2+} homeostasis emerged after the crystal structure of parvalbumin was discovered by Kresinger in 1972 (Nockholds et al., 1972). This discovery was the first among a family of proteins referred to as EF-hand proteins. EF-hand proteins function to buffer Ca^{2+} and decipher information. EF-hand proteins are the most abundant motif among animals (Carafoli, 2002; Chazin, 2011; Bagur et al., 2017). The term "EF-hand" originates from the structural orientation of the two alpha helices (E and F) that form together with a conserved Ca^{2+}-binding region of amino acids. Affinities vary among EF-hand domain proteins based on the composition of amino acids within the binding region (Lewit-Bentley et al., 2000). Another example of a highly conserved protein containing EF-hand domains is centrin. Centrin is a Ca^{2+} -binding protein with four Ca^{2+} -binding EF-hand domains and is present at the base of the cilium, the basal body (Figure 4B; Taillon et al.,1992). The presence of such conserved Ca^{2+} binding proteins at the base of the cilium raises the question: How do these proteins interact with intracellular $Ca^{2+}$and facilitate transfer of Ca^{2+} to and from the ciliary compartment?

Ca^{2+} buffering organelles and the transfer of Ca^{2+}

Aside from proteins, cells possess internal structures capable of storing and releasing Ca^{2+}. Two of the most studied Ca^{2+} storage organelles include the endoplasmic reticulum (ER) and the

mitochondria. The storage of Ca^{2+} in organelles ensures that cells have stored Ca^{2+} to meet the needs of the cell. Cytosolic Ca^{2+} is subject to fluctuations depending on the state of the cell. The concentration of Ca^{2+} in the cytosol can vary, but typically rests at between 100-500nM. Cell stimuli such as membrane depolarization can cause a rapid influx of extracellular $Ca^{2+}$and result in Ca^{2+}levels within the cell to increase (Bagur et al., 2018). When Ca^{2+} within the cytosol is released in response to depolarization, there is a rapid influx of extracellular Ca^{2+} through Ca^{2+}channels that line the plasma membrane or internal Ca^{2+} stores. Most often the release of $Ca^{2+}$from internal calcium stores is a product of the activation of IP3 receptors (IP3R) and ryanodine receptors (RyR) (Bagur et al., 2018). When Ca^{2+} levels are too high in an area of the cell, the ER and mitochondria can uptake excess Ca^{2+} from the cytosol and return the cell back to resting Ca^{2+} levels. A return to resting cytosolic Ca^{2+} levels is important to the cell because Ca^{2+} can modulate processes such as gene expression, muscle contraction and metabolism (Bagur et al., 2018). Ca^{2+} levels within the cell must be precise for cell signaling and internal Ca^{2+} stores such as the ER, mitochondria, and Golgi play a crucial role in the release and reuptake of Ca^{2+} to accomplish such functions.

The spatial relationship between the ER and mitochondria has been characterized and shown to form contact points called Mitochondria-ER contact sites (MERCS; Rieusset, 2018). These specialized contact points can directly facilitate Ca^{2+} transfer (Kaufman et al., 2014). The direct contact or close proximity of prominent of these two Ca^{2+} storage organelles for the exchange of Ca^{2+}suggests that other Ca^{2+} storage organelles such as the Golgi may facilitate Ca^{2+} transfer at other organelles as well. Since Ca^{2+} transfer can occur between membrane-bound organelles, this suggests the possibility that Ca^{2+} transfer may also occur between a membrane-bound organelle

and a non-membrane-bound organelle. Considering that the base of the cilium is not separated from the rest of the cell by a limiting membrane, Ca^{2+} from membrane organelles should be able to reach the ciliary compartment.

The Golgi is involved in intracellular protein trafficking and Ca^{2+} signaling. Golgi-mediated Ca^{2+} signaling relies on Ca^{2+} channels that rapidly release Ca^{2+} to the microenvironment surrounding the Golgi (Micaroni et al., 2012). Unpublished research from the Galati lab shows that cilia can be variably positioned with respect to the Golgi. Approximately 92% of cilia from individual 3T3 cells are closer than 2μm to the Golgi (Josh McNamara, personal comm.). Since Ca^{2+} travels across the cell as dissipating waves that travel at ~ 5 mm/s, Ca^{2+} released from the Golgi may differentially impact cilia that are well separated from the Golgi (Jaffe et al., 2010). The Golgi is capable of modulating other subcellular complexes and organelles. Similar to the contact points formed from the mitochondria and the ER, the Golgi can form contact points with the ER for the transfer of lipids as well as ions such as Ca^{2+} (Pizzo et al., 2011; Mesmin et al., 2018). It is hypothesized that Ca^{2+} gradients originating from the Golgi may be involved with stabilizing and regulating the timing of vesicle uncoating (Ahluwalia et al., 2001). It is currently unclear whether cilia respond to similar Ca^{2+} signaling events from differential Ca^{2+}gradients originating from the Golgi.

The intraflagellar transport protein, IFT20 is a Golgi complex protein that is required for cilia assembly. Strong knock-down of IFT20 in mammalian cells blocks the formation of cilia but leaves the Golgi intact (Follit et al. 2006). Ciliogenesis requires IFT (i.e., intraflagellar transport) mediated transport for the transport of cilia and membrane associated proteins into the ciliary

compartment (Kozminski et al., 1993; Lechtreck, 2015; Figure 5). When cilia are being assembled, IFT20 mediates this process with bidirectional movement up (i.e., anterograde) and down (i.e., retrograde) along the cilium (Figure 5). This process relies on the motor proteins kinesin-2 for anterograde movement and dynein-2 for retrograde movement (Lechtreck 2015). When proteins reach the ciliary tip via anterograde movement, some protein cargo is released followed by IFT20 reorganizing and returning to the basal body via retrograde movement. BBsome is a protein complex associated with transporting specific cilia membrane proteins via IFT mediated transport (Nachury et al., 2007; Williams et al., 2014) BBsome is involved in the assembly and stabilization of IFT20 cargo (Williams et al., 2014). BBsomes are not required for cilia to form, but mutations associated with this protein complex can cause Bader-Biedl syndrome (i.e., BBS), which can have effects including obesity, blindness, cardiomyopathy and kidney anomalies (Blacque et al., 2004; Lechtreck 2015). Tubulin is another protein that enters the cilium to form microtubules (Craft et al., 2015). Cilia in *Chlamydomonas reinhardi* and *Tetrahymena thermophila* have been shown to shorten when IFT mediated transport is inhibited, suggesting that it is important for maintaining cilia (Lechtreck et al., 2013). Cilia disassemble prior to mitosis, but the involvement if IFT mediated transport is unclear (Engel et al., 2012). The IFT20 dependent cargo trafficking of cilia bound proteins is essential for cilia to form, without this system, cilia are unable to have cilia associated proteins localized to the ciliary compartment or ciliary membrane and therefore cilia do not form. The requirement of a Golgi associated protein in cilia formation poses questions as to what other interactions the two organelles share.

The spatial configuration of cilia in relation to the Golgi can also impact cilia function and sensation. Vertebrate non-motile cilia can be submerged in a deep membranous pit that is created though membrane invagination around the base of the cilium. Cilia that are surfaced (i.e., not submerged) carry a shallow pit or pocket at the base (Mazo et al., 2016). Cilia that remain submerged are typically found in cells that do not display apical-basal polarity (Galati et al. 2016). When cilia are submerged and proximal to the Golgi, they are unresponsive to fluid flow (i.e., mechanosensation). Conversely, cilia separate from Golgi respond to fluid flow. In addition to mechanosensation, cilia that extend from the cell surface and are located away from the Golgi can recruit the Shh components, Smoothened and Gli2, in the absence of Shh stimulation (Galati et al. 2016; Mazo et al. 2016). Since Golgi proximity impacts ciliary function, investigating ciliary Ca^{2+} in conjunction with Golgi proximity will potentially reveal a new mechanism that explains how interactions between Golgi and cilia impact ciliary function. In addition to spatial configuration, the structure of cilia further suggests interaction with Ca^{2+}originating from inside the cell.

Current model of ciliary Ca^{2+}

Structurally, the base of the cilium is enriched with evolutionarily conserved Ca^{2+}-binding proteins (Figure 4B; Laoukili et al., 2000). Cilia maintain a higher concentration of Ca^{2+} relative to the cell; however, questions remain as to how this environment is maintained. Unlike the Ca^{2+} sequestering organelles previously discussed, which have membranes to keep their Ca^{2+} isolated from the outside environment, cilia lack a membrane to separate ciliary Ca^{2+} from the rest of the cell. The current model on cilia Ca^{2+} homeostasis was proposed by Delling et al. 2013 after experiments conducted on human retinal pigment epithelial cells (i.e., hTERT RPE-1). Their

findings suggest that cilia maintain a functionally distinct Ca^{2+} environment from the cytoplasm, regulated by a favorable influx/efflux ratio. This influx/efflux ratio is considered to be maintained by many Ca^{2+} permeant channels or other ion channels/transporters that line the ciliary membrane (Figure 4A). The channels and transporters are thought to maintain high Ca^{2+} levels easily due to the small volume of the cilium relative to the rest of the cell. The model can be simplified as an analogy provided by Delling et al. 2013 that the Ca^{2+} within the cilium is like a water tower connected to a large lake representing the cytoplasm by a small pipe (i.e., basal body). Since Ca^{2+} is higher in cilium compared to the cytoplasm, Ca^{2+} diffuses from the cilium to cytoplasm, but not cytoplasm to cilia (Delling et al., 2013). Based on this model, one would predict that Ca^{2+} should diffuse freely into cilia when the Ca^{2+} gradients are reversed, and the cytoplasm increases to a Ca^{2+} concentration greater than the cilium (Figure 4C).

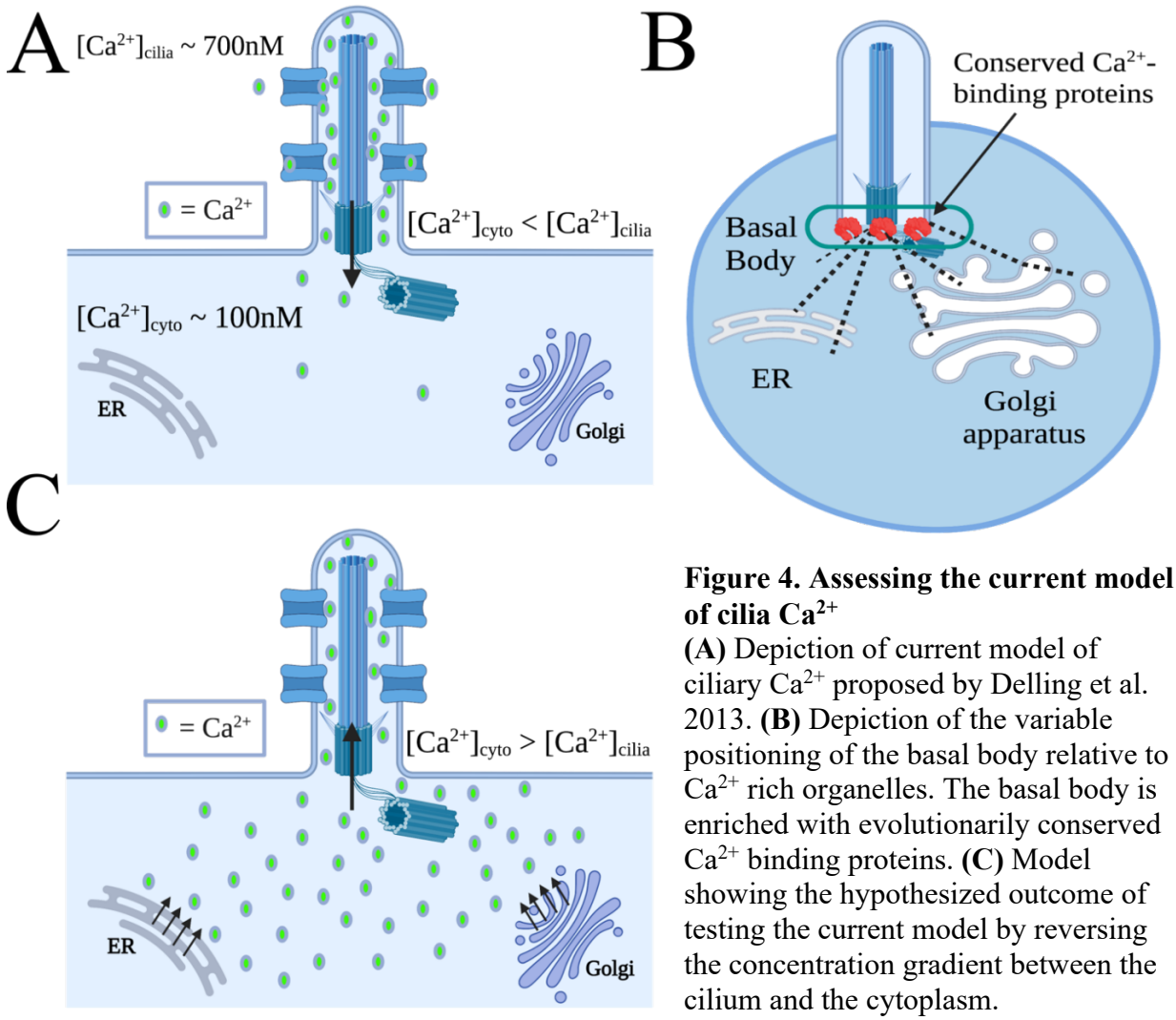

Figure 4. Assessing the current model of cilia Ca^{2+}
(A) Depiction of current model of ciliary Ca^{2+} proposed by Delling et al. 2013. **(B)** Depiction of the variable positioning of the basal body relative to Ca^{2+} rich organelles. The basal body is enriched with evolutionarily conserved Ca^{2+} binding proteins. **(C)** Model showing the hypothesized outcome of testing the current model by reversing the concentration gradient between the cilium and the cytoplasm.

The current "outside-in" model, suggests that cilia maintain higher concentrations of Ca^{2+} by a steady influx of Ca^{2+} into cilia from outside of the cell through Ca^{2+} channels lining the outside of the cilia (Figure 4A; Delling et al., 2013). However, this model fails to consider the Ca^{2+} buffering organelles that are often found near cilia (Figure 4B). Whether spatial configuration of these Ca^{2+} buffering organelles (Golgi, ER, and/or mitochondria) relative to cilia impacts ciliary Ca^{2+} has not been investigated (Figure 4B). Since these Ca^{2+}-buffering organelles can modulate each other's Ca^{2+}environment, they may be capable of modulating Ca^{2+} at other cellular structures such as the cilium, which is not separated from the rest of the cell by a limiting membrane. The existing evidence linking the spatial relationship between cilia and the Golgi to cilia function as well as the requirement of the Golgi complex protein, IFT20, for ciliogenesis, leaves many unanswered questions about the intricate networking between these two organelles. With live-cell imaging techniques, we aim to uncover the impact of disrupting the structural integrity of the Golgi on cilia Ca^{2+} and whether Ca^{2+} originating from the Golgi is capable of reaching the cilium.

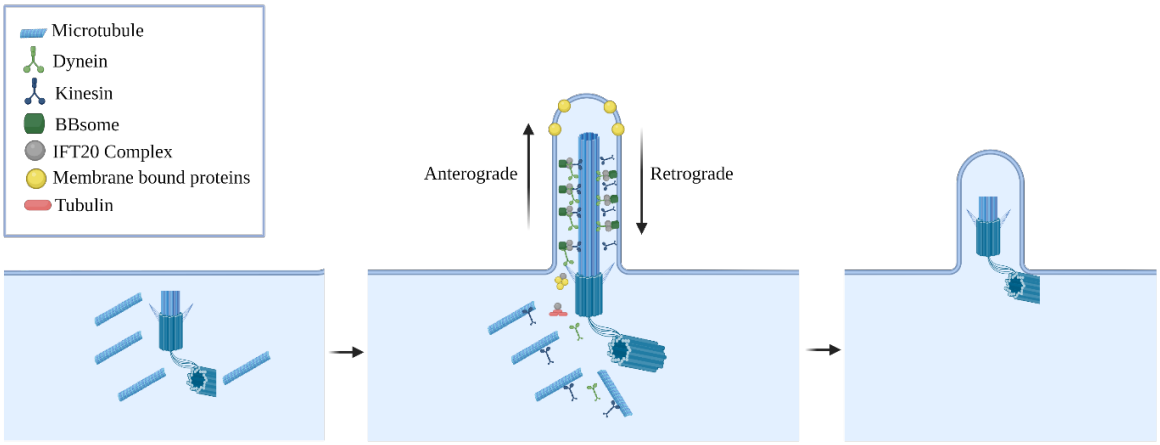

Figure 5. IFT20 is required for ciliogenesis
Schematic displaying ciliogenesis. The first panel depicts cilia assembly as the mother and daughter centriole dock to the plasma membrane to form the basal body. Next, IFT20 along with kinesin direct the upward (i.e., anterograde) movement of cilia bound protein complexes. When these proteins move down the cilium (i.e., retrograde), dynein directs the movement. Incoming cargo into the cilium includes tubulin, membrane bound proteins, BBsome proteins, and other cilia associated proteins. The final panel depicts cilia disassembly.

Part II – Background on the tools needed to evaluate the relationship between intracellular Ca^{2+} storage organelles and cilia

Measuring Ca^{2+} in cilia of live cells

To evaluate Ca^{2+} in cilia and the cytoplasm in living cells (i.e., *in vivo*) genetically encoded Ca^{2+} indicators (GECI) can be localized to subdomains within the cell. Ciliary targeting of such GECIs has been achieved by fusing them to Arl13b (ADP Ribosylation Factor Like GTPase 13B), a protein that localizes to the inner leaflet of the ciliary membrane (Delling et al., 2013; Higginbotham et al., 2012). The most advanced GECI for Ca^{2+} measurements is GCaMP6, which was initially developed in 2001 and optimized over many iterations (Nakai et al., 2001; Akerboom et al., 2012). GCaMP has been used in many areas of research including characterizing activity in neuronal populations in the motor cortex (Tian et al., 2009) and hippocampus (Dombeck et al., 2010). GCaMP is comprised of three domains: calmodulin, green fluorescent protein, and M13. Calmodulin (CaM), a highly conserved Ca^{2+} binding protein, is located at the C-terminus. Green fluorescent protein (GFP), a protein that emits green fluorescence, is in the center. M13, a domain isolated from myosin light-chain kinase, is located at the N-terminus. When Ca^{2+} is present, Ca^{2+} ions bind to the CaM domain, which causes a conformation change and subsequent binding to the M13 domain. This conformation change initiates a deprotonation that stabilizes the fluorophore located in the core of GFP, resulting in fluorescence (Figure 6B; Wang et al., 2008). In the plasmid used to quantify Ca^{2+}, GCaMP6 is fused to the Ca^{2+} insensitive protein, mCherry (Figure 6A). The fusion of these two proteins is essential to ratiometric imaging as mCherry normalizes the signal from the GCaMP reporter since mCherry does not change in the presence of Ca^{2+} (Figure 6B). Without ratiometric

imaging, Ca^{2+} cannot be measured accurately because increased GECI fluorescence could be due to an increase in the number of GECI molecules or an increase in Ca^{2+}. Although Förster or fluorescence resonance energy transfer (FRET)-based GECIs can infer Ca^{2+}, GCaMP is optimal due to its better signal to noise ratio and increased photostability (Tian et al., 2009).

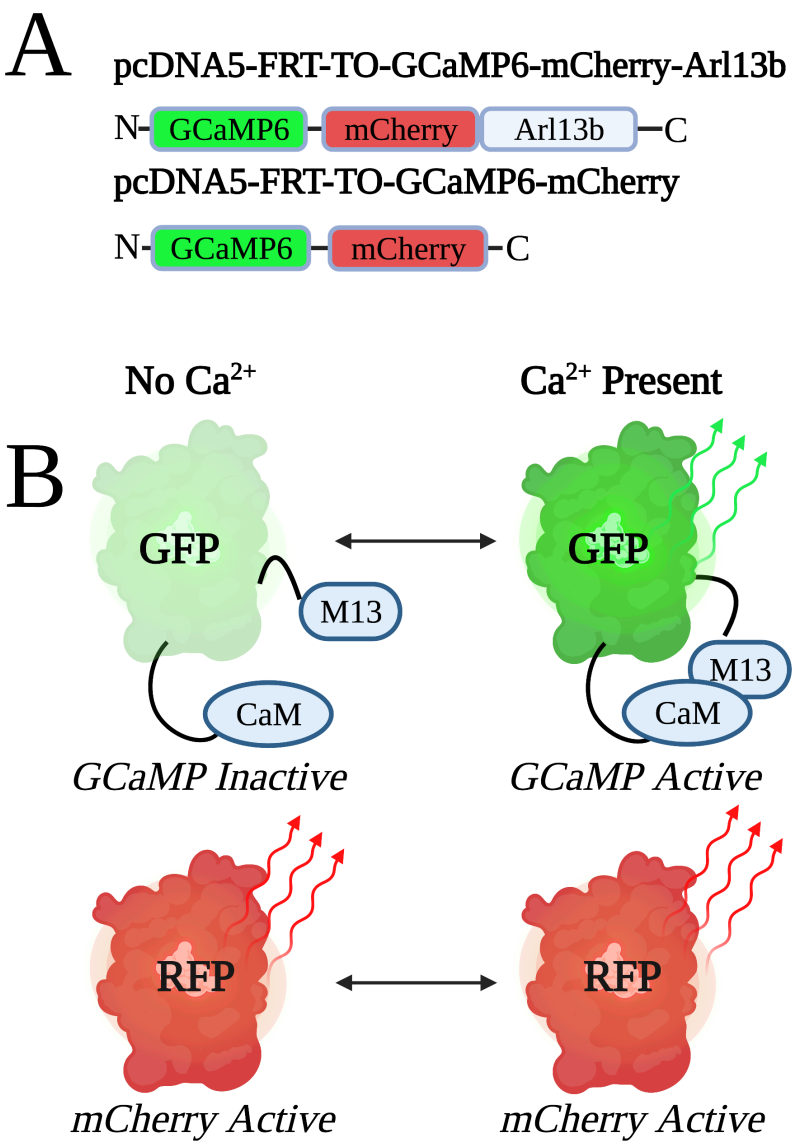

Figure 6. The fusion of GCaMP6 and mCherry allows for the detection of Ca^{2+} during live-cell imaging
(A) Depiction of the construct used for measuring Ca^{2+} in cells *in vivo* through ratiometric imaging. **(B)** GCaMP6 is sensitive to Ca^{2+} while mCherry is in-sensitive to Ca^{2+}. The two proteins can be used to calculate a ratio using the fluorescence intensity of GCaMP6/mCherry to get a ratio representing relative levels of Ca^{2+}.

Pharmacology of Ca^{2+} release and the integrity of the Golgi

The broad application of small molecule drugs that target Ca^{2+} storage organelles (i.e., pharmacology) can be used to evaluate how calcium storage organelles impact ciliary Ca^{2+}. Brefeldin A (BFA) is a small hydrophobic molecule produced by the toxic fungi Penicillium brefeldin that disrupts protein trafficking from the ER to the Golgi leading to Golgi fragmentation and dispersal (Chardin et al., 1999; Fujiwara et al.,1988). Due to the established relationship between the Golgi and the cilium, BFA can be used to determine if the dispersal of the Golgi impacts ciliary Ca^{2+}. Histamine is a bioactive compound that induces inositol 1,4,5-trisphosphate (IP3)-mediated Ca^{2+} release in 3T3 cells by acting as an agonist for H1 receptors within the ER and Golgi membranes (Figure 7; Aguilar-Maldonado et al., 2003). Thapsigargin is a small molecule found in *Thapsia garganica L*. that inhibits SERCA ATPase pumps responsible for the reuptake of Ca^{2+} into intracellular Ca^{2+} storage organelles (Figure 7; Jaskulska et al., 2020; Wictome et al., 1992). Therefore, treating cells with a combination of histamine and thapsigargin can stimulate sustained Ca^{2+} release from intracellular stores. Cilia Ca^{2+} levels are thought to be sensitive to mechanical stimulation due to Ca^{2+} entry from extracellular sources, which can occur during pharmacology experiments. One way to discern whether the source of a Ca^{2+} influx is from mechanical stimulation (i.e., extracellular source) or from the histamine and thapsigargin co-stimulation (i.e., intracellular source) is to use a Ca^{2+} channel blocker that will inhibit calcium from entering from the extracellular environment. Lanthanum chloride (i.e., $LaCl_3$; lanthanum) is a non-specific extracellular Ca^{2+} antagonist that blocks extracellular Ca^{2+} from entering the cytoplasm and ciliary membrane. $LaCl_3$ accomplishes this by blocking calcium channels in the permeation pathway of the channel (Tsien et al., 1987). Lanthanum is part of a family of cation Ca^{2+} channel blockers such as cadmium, cobalt, and nickel which all block Ca^{2+}

channels by binding in the permeation pathway of the pore (Tsien et al., 1987; Mlinar and Enyeart., 1993). These transition metals accomplish this by competing with Ca^{2+} for the permeation pathway and having similar ionic radii to Ca^{2+} (Nachshen, 1984).

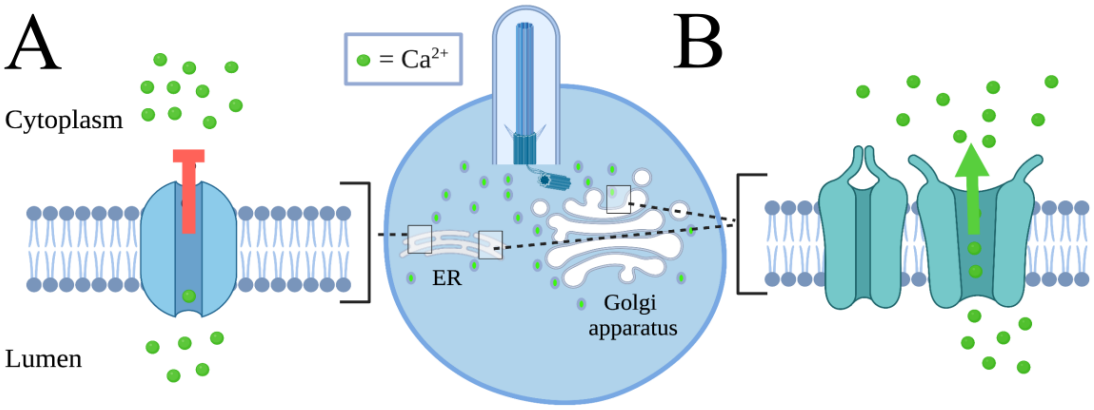

Figure 7. Stimulating intracellular Ca^{2+} release to evaluate cilia response
(A) Depiction of thapsigargin mechanism blocking rapid Ca^{2+} reuptake by the ER. **(B)** Depiction of histamine mechanism by which it activates the IP3 pathway through interactions with H1 receptors. This activation initiates Ca^{2+} release from the ER and Golgi into the intracellular environment (i.e., cytoplasm).

Overview of transient transfection experiments

To express the Arl13b-GCaMP6-mCherry fusion protein, transient transfection was used to introduce transgenes into mammalian cells. During transient transfection, a lipofectamine reagent is commonly used to generate a cationic lipid complex around the transgene-containing DNA plasmids. Ultimately, the DNA/lipid complex enters the cell via endocytosis, a process by which an invagination of the cell surface occurs to form an intracellular membrane-bound vesicle. Once inside the cell, the plasmids are released and travel to the nucleus to undergo transcription into mRNA (24-96 hr.; Figure 8). To study cellular Ca^{2+}, cells expressing Ca^{2+} reporters were imaged using widefield epifluorescence microscopy. Data collected from these sessions were quantified using the open-source image processing software, Fiji. To streamline and standardize quantification, custom Java-based code was written. Image analysis code utilized tools to measure the pixel intensity of GCaMP6 and to normalize this signal to the pixel intensity of mCherry. To ease obstacles for future experiments, a stable cell line was produced. A stable cell line is a line of cells that permanently express a given protein of interest at stable levels.

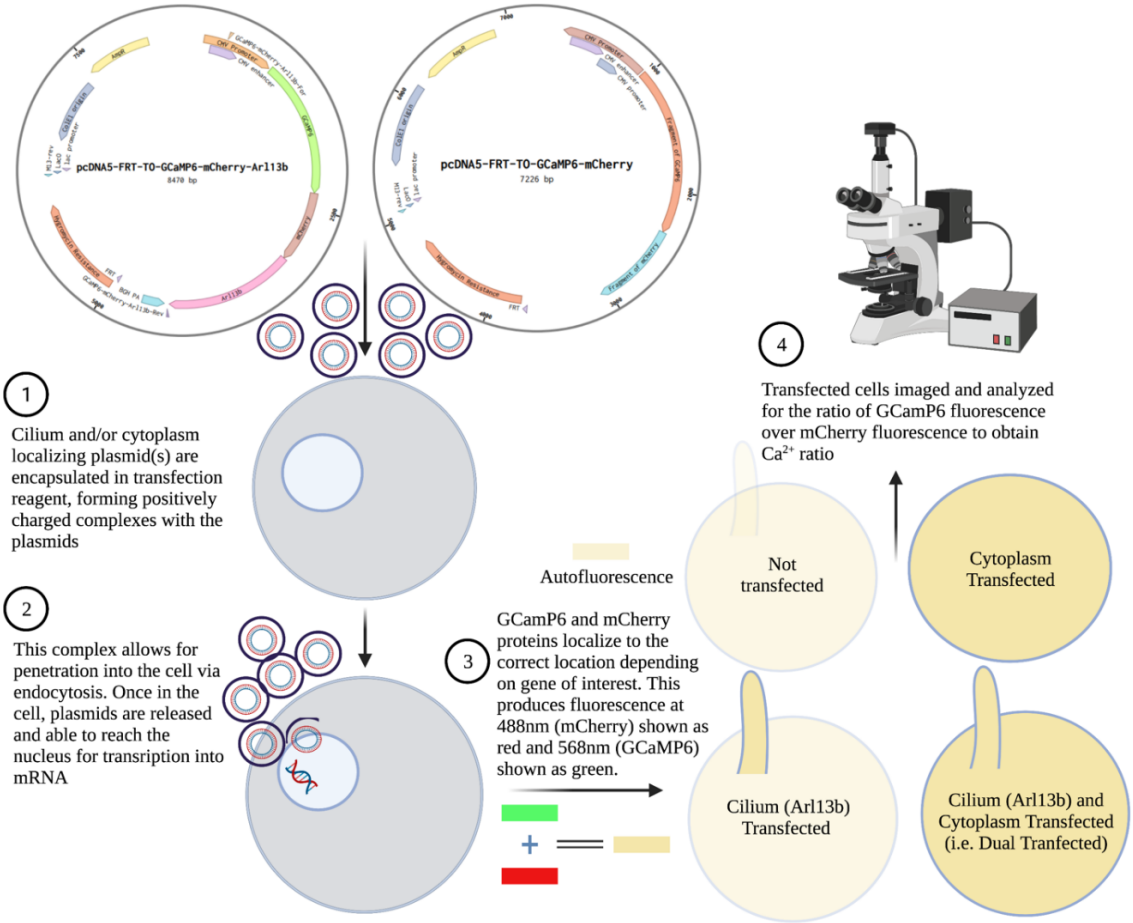

Figure 8. Transient transfection workflow for ratiometric Ca^{2+} imaging assay
Process of transient transfection using the jetPRIME DNA transient transfection kit with plasmids targeting the cytoplasm or cilia (Arl13b).

Summary

The goal of this research was to identify whether cilia Ca^{2+} levels are influenced by the surrounding intracellular environment; specifically, their positionality relative to other Ca^{2+}-rich organelles. To answer this question, pharmacology was utilized to induce changes in intracellular Ca^{2+}. Due to studies in 2016 that established a functional spatial relationship between the Golgi and cilia, the Golgi was the first target (Mazo et al., 2016). While the Golgi is critical for modulating Ca^{2+} in the cell, other organelles such as the ER may be involved. Initially, an assay utilizing BFA to disrupt Golgi structure while measuring Ca^{2+} in cilia was conducted. To further investigate the role of the Golgi in ciliary Ca^{2+}, the small molecule drugs, histamine and thapsigargin, were used to initiate a rapid, sustained Ca^{2+} flux. Lastly, experiments utilizing $LaCl_3$, a Ca^{2+} blocker that blocks Ca^{2+} channels on the plasma membrane were conducted to evaluate the impact of mechanical stimulation on ciliary $Ca^{2+}$and whether the source of Ca^{2+} flux could be discerned. Together, these experiments provide the framework to increase our understanding of whether cilia Ca^{2+} levels fluctuate in response to intracellular Ca^{2+} derived from a local physiological source. One limitation to this approach, however, was the inherently low throughput of transient transfections. To overcome this limitation, a stable cell line that constitutively expresses the cilium Ca^{2+} reporter was generated.

Collectively, this research seeks to illuminate how an evolutionarily ancient structure, the cilium, has integrated into evolutionarily ancient Ca^{2+} signaling pathways. Specifically, this work tested a new "inside-out" model of ciliary Ca^{2+} homeostasis by examining the spatial coupling between the base of the cilium and Ca^{2+} rich organelles using live-cell fluorescent imaging. Uncovering the mechanisms in which cilia maintain Ca^{2+} will contribute to our knowledge of intracellular

coordination of Ca^{2+}, a process critical for cellular communication, development, and human health. This work addresses a perplexing and fundamental question: How does the cilium, which is not separated from the cytoplasm by a limiting membrane, integrate into a larger network of membrane-bound regulators of intracellular Ca^{2+} homeostasis?

Methods

Cell culture

NIH 3T3 cells were used as the parent cell line for all experiments. This cell line was established from primary mouse embryonic fibroblast cells and was purchased by the Galati lab from the ATCC repository (CRL-1658). All cells were free of mycoplasma contamination. NIH 3T3 cells were cultured in DMEM (Corning® DMEM [+] 4.5 g/L glucose, L-glutamine, sodium pyruvate, VWR45000-304) + 10% bovine calf serum (VWR SH30073.04IR). All cells were kept in the Galati Lab incubator at 37°C and 5% CO_2. Cells were passaged every 3-4 days to maintain cells between 10-90% confluency.

Transient transfection

Cells were transfected using the jetPRIME DNA transfection reagent kit from Polyplus to introduce pcDNA5-FRT-TO-GCaMP6-mCherry-Arl13b for cilia localization and/or pcDNA5-FRT-TO-GCaMP6-mCherry for cytoplasm localization. The transfection mixture was applied to cells plated on 24 mm round coverslips glass coverslips in DMEM + 10% calf serum at 60% confluency. In order to remove potential endotoxins and/or residual transfection reagent, media was changed 6 hours post-transfection. Cells continued to grow after transfection and were imaged 24-48 hours post-transfection. Imaging times varied between 24-48 hours due to cell growth rate variability and whether cilia were present or not. Cilia formation was encouraged by allowing cells to reach confluency prior to imaging.

Microscopy

Cells were imaged on a Nikon Eclipse Ti2 E microscope with a fast-switching 4-channel LED illumination source and a high-speed Photometrics Prime95b sCMOS camera. GCaMP was excited with 488nm LED. mCherry was excited with 568nm LED. Both GCaMP and mCherry emission was collected through a quad-pass emission filter (Chroma). The microscopy acquisition was controlled through Micro-Manager 2.0. 24mm round coverslips containing confluent cells were attached to an Attofluor Cell Chamber (ThermoFisher). HBSS containing Ca^{2+} (1.26mM) used as imaging media. All cells utilized in experiments were pre-incubated in 900uL HBSS 30 min prior to imaging to acclimate cells and prevent artifacts from sudden environmental changes. All incubations took place in the incubator at 37°C and 5% CO_2. Cell imaging was performed at room temperature and within 5 minutes of cells coming out of the incubator.

Image analysis

All images were analyzed using the application FIJI with custom-made code to determine the pixel intensity of the fluorescent reporters, GCaMP6 and mCherry (Figure 9). This code was designed to assign the location of cilium by taking the derivative of the pixel intensity in the area selected. This method can identify the bright borders of the cilium. F GCaMP6/F mCherry ratios were determined by taking the total average pixel intensity GCaMP6 divided by the total average pixel intensity of mCherry for the cilium identified. Cytoplasm measurements were manually selected using the region of interest (ROI) box tool. Cytoplasm ROIs were selected near the base of the cilium and the measurement value was determined by the developed code reporting the average pixel intensity within the ROI square. Ca^{2+} ratios for the cytoplasm were determined by taking the total average pixel intensity GCaMP6 divided by the total average pixel intensity of

F GCaMP6/ F mCherry Ratio Analysis Code Overview

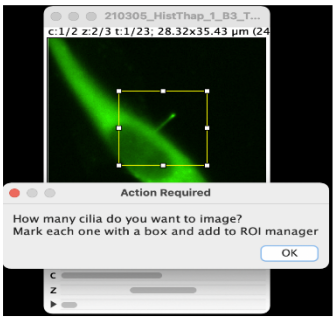

1. Select cell(s) to analyze

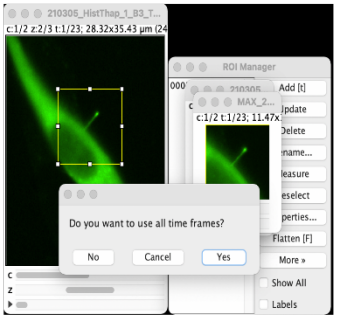

2. Check to see if cell shifts out of focus

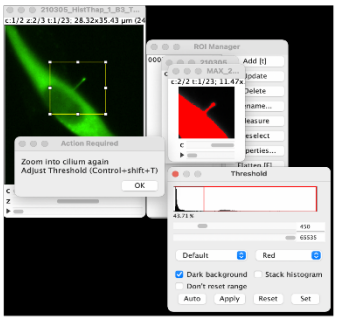

3. Adjust image theshold to identify cilium marigins

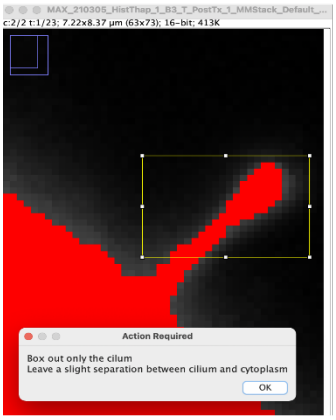

4. Select region of cilium to measure

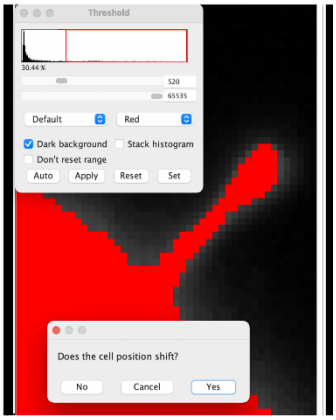

5. Verify that ROI box contains cilium for all frames

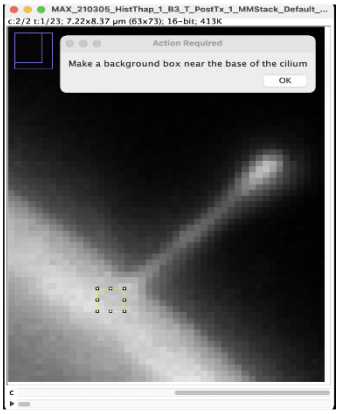

6. Select ROI for cytoplasm measurements

Label	Cilia GCaMP	Cilia Cherry	Cilia Ratio	Cyto GCaMP	Cyto Cherry	Cyto Ratio
time_1	562.521	727.397	0.773	717.812	1269.688	0.565
time_2	560.257	725.257	0.772	709.562	1286.875	0.551
time_3	571.257	748.043	0.764	711.188	1290.562	0.551
time_4	671.795	749.051	0.897	834.625	1217.188	0.686
time_5	799.667	714.107	1.120	1854.125	1371.625	1.352
time_6	773.690	698.873	1.107	2070.375	1400.000	1.479
time_7	641.583	641.467	1.000	1649.125	1381.750	1.194
time_8	574.172	613.966	0.935	1296.812	1385.125	0.936
time_9	566.814	653.983	0.867	1157.438	1380.312	0.839
time_10	583.222	668.524	0.872	1122.188	1359.438	0.825
time_11	597.776	679.672	0.880	1135.750	1343.875	0.845
time_12	597.904	678.616	0.881	1155.875	1380.375	0.837
time_13	582.435	658.918	0.884	1161.938	1359.938	0.854
time_14	573.227	660.413	0.868	1124.125	1368.875	0.821
time_15	557.179	659.192	0.845	1112.188	1400.500	0.794
time_16	567.773	677.307	0.838	1095.250	1419.750	0.771
time_17	528.866	665.985	0.794	1033.750	1444.062	0.716
time_18	500.242	648.409	0.771	951.062	1426.000	0.667

7. Code measures pixel intensity of each channel, GCaMP and mCherry, over time. Pixel intensity of GCaMP is divided by the pixel intensity of mCherry for ratio.

Figure 9. F GCaMP6/ F mCherry analysis code overview
Summary of each step of code used in FIJI to calculate F GCaMP6/ F mCherry. Full code available by request.

mCherry for the ROI identified. The code developed in FIJI to obtain Ca^{2+} ratios is open source and available upon request.

Pharmacology

1.0μM Brefeldin A (BFA) was used to disperse the Golgi. BFA was purchased from BioVision (1560-5) and reconstituted in DMSO. After a 30-minute incubation period, cells were imaged for 30 minutes at 1-minute intervals. Cells were held in the incubator at 37°C and 5% CO_2 during 30-minute BFA incubation step. Cells were exposed to a final concentration of 1.0 μM .100μM histamine was used to induce intracellular Ca^{2+} release. Histamine was purchased through Cayman Chemicals (33828) and reconstituted in water. Drug was delivered in conjunction with thapsigargin. 100μM thapsigargin was used to aid in intracellular Ca^{2+}release by restricting the reuptake of Ca^{2+} into the ER. Thapsigargin was purchased through Cayman Chemicals (10522) and reconstituted in DMSO. For experiments using histamine and thapsigargin, the vehicle control consisted of water and DMSO. 100μL histamine and thapsigargin were added to the imaging chamber after three pre-treatment images. Cells were then imaged for 3 minutes at 30-second intervals to limit phototoxicity. Images were analyzed for F GCaMP6/F mCherry intensity ratios to infer Ca^{2+} levels at each time interval. $LaCl_3$ was used at a final concentration of 1mM. Lanthanum (III) Chloride Hydrate was purchased from Sigma-Aldrich (20211-76-1) and reconstituted in water. Water was used as the vehicle control for $LaCl_3$ experiments.

Mechanical Stimulation Assay

The mechanical stimulation experiment utilized a P200 pipette set to 100μL to generate hydrodynamic force to mechanically stimulate cilia during live-cell imaging. Pipette was drawn

up and down three times inside HBSS within the image chamber and cells were imaged for three minutes at 30 second intervals. Stimulation was repeated after 3 minutes of imaging with another 3 minutes of imaging at 30 second intervals. Each frame of each captured image was carefully assessed to ensure that the cilium remained in focus after mechanical disturbance.

Cloning and Cell Line Workflow

The plasmid pH2b-emiRFP670 was purchased from Addgene (Plasmid #136571) and was used as the template for the vector as it contains a neomycin mammalian selection marker. A fragment containing the fluorescent reporter from pH2b-emiRFP670 and part of pH2b was removed. Additionally, a fragment containing GCaMP6-mCherry-Arl13b was inserted into the vector that partially contained pH2b. Plasmid fragments were generated by PCR after failed attempts with restriction enzyme cloning. The fragment containing Arl13b was amplified using PCR including a NdeI on the 5' end and NotI on the 3' end (Figure 18A). The fragment containing the pH2b vector was amplified with PCR including a Ndel site on the 5' end and NotI on the 3'. The insert (Arl13b) was ligated into the vector (pH2b) and screened by transforming DH5alpha cells and observing growth in the presence of ampicillin. The correct insert orientation was confirmed by restriction digestion (Figure 18B). The new plasmid then conferred antibiotic resistance for neomycin and could be used for stable transfection and subsequent antibiotic selection. G418, an analogue of neomycin, was purchased through ThermoFisher Scientific (J62671).

To create a stable cell line, NIH 3T3 cells for stable cell line were transfected using the same jetPRIME reagent protocol as previous experiments, however, the media change at 6 hours post-transfection also included G418, an antibiotic used for the selection of neomycin resistant cells.

Cells were kept in 600µg/mL G418, a concentration verified to work in the cell line used with an initial kill curve experiment (Figure 19A). A non-transfected control was also included for comparison both with and without G418. Expression from transient transfection typically lasts 24-96 hours, therefore cells were kept from confluency by passaging within the 96-hour window. Transfected cells that survived the 96-hour window were expanded into multiple 6-well plates. Each well that contained surviving cells was expanded into two wells of a 6-well plate, one well kept at 600µg/ml and another 800µg/ml G418. The concentration of G418 was increased to lower the likelihood of any non-transfected cells growing in the dish. A control cells were kept at 600µg/ml to be safe since Arl13b is not a highly expressed gene. In this case, because Arl13b is not highly expressed, there is an increased risk that the antibiotic concentration will be too high and kill the cells due to the newly acquired neomycin resistance being expressed at low levels. Cells were monitored daily for cell death and changes in cell morphology. Test coverslips on expanded cells revealed that a subpopulation of cells had integrated the plasmid and expressed GCaMP6-mCherry in cilia. 12-days post-transfection, G418 was dropped to 400µg/ml to minimize cell stress for the subsequent steps. The polyclonal cells required further selection to generate a functional stable monoclonal cell line. Limiting dilutions were used to isolate monoclonal colonies and clones displaying expression were selected and expanded using 10 96-well plates, equating to 160 possible clones. A final 96-well plate with a glass bottom was used to screen for monoclonal cell populations that had expression of GCaMP6-mCherry-Arl13b (Figure 20).

Results

Establishing a method to measure cilia Ca^{2+} *in vivo*

NIH 3T3 cells are a standard model for studying primary cilia formation and Shh signaling, however, cilia Ca^{2+} levels have not yet been assessed in NIH 3T3 cells. To monitor cilia Ca^{2+} levels *in vivo*, a genetically encoded Ca^{2+} sensor, GaMP6, was expressed and localized to cilia. For sensor localization, transient transfection was used to deliver the plasmid pcDNA5-FRT-TO-GCaMP6-mCherry-Arl13b for cilia localization (Figure 10). To determine if cilia from NIH 3T3 cells exhibit the same Ca^{2+} dynamics as the cells used in establishing the current model of ciliary Ca^{2+}, hTERT-RPE1 cells, a collection of steady state (i.e., baseline) Ca^{2+} levels were measured (Figure 10B).

To calculate GCaMP6/mCherry ratios, the fluorescence intensity of the Ca^{2+}-sensitive protein, GCaMP6, was divided by the fluorescence intensity of the Ca^{2+}-insensitive protein, mCherry. Images containing ratiometric data were acquired through live-cell imaging, and these images were quantified using a custom-made code in the image analysis software, FIJI (Figure 9). Briefly, this semi-automated code streamlined the data analysis workflow to ensure consistent and accurate measurements by recognizing cilia margins and using thresholding to remove parts of the image that should not be included in the analysis (i.e., background). This code is also applied to measure Ca^{2+} levels in the cytoplasm by positioning an ROI near the base of the cilium, avoiding the non-transfected nucleus. The ultimate output of the code is a series of GCaMP6 fluorescence intensities normalized to mCherry fluorescence intensity, which we define as F GCaMP6/ F mCherry. Baseline NIH 3T3 cilia Ca^{2+} levels were then be compared to that of previously published results in hTERT-RPE1 cells (Delling et al., 2013; Figure 10).

Results from NIH 3T3 cells were consistent with hTERT-RPE1 cells used in Delling et al. 2013. Specifically, NIH 3T3 cilia exhibit higher Ca^{2+} levels than the cytoplasm. The average ciliary Ca^{2+} ratio was 1.032 while the average cytoplasmic Ca^{2+} ratio was 0.897 (Figure 10B). In a population of 115 cilia measured over 27 different coverslips, the standard deviation was 0.153. Cytoplasm measurements of 90 cells over 24 different coverslips displayed a standard deviation of 0.202 (Figure 10B). These results suggest that NIH 3T3 cells display similar baseline Ca^{2+} dynamics as cells used to establish the current model of ciliary Ca^{2+}, hTERT-RPE1 cells.

Effects of Golgi structural disruption on cilia Ca^{2+}

To first evaluate whether the Golgi can influence cilia Ca^{2+} signaling, the spatial coupling of the cilium relative to the Golgi was examined. In many cell types, the base of the cilium is embedded within the Golgi. Unpublished data from the Galati lab show that 92% of cilia from individual cells are closer than 2 μm from Golgi in NIH 3T3 cells (Josh McNamara, personal comm.). Cilia were classified as either "close" (less than 2 μm between cilium and Golgi) or "far" (greater than 2μm between cilium and Golgi) (Figure 11A). Whether separation between the cilium and the intact Golgi impacts cilia Ca^{2+} signaling is not clear. If the Golgi influences cilia Ca^{2+} signaling, disrupting the Golgi should impact cilia Ca^{2+} levels. To test this possibility, cilia Ca^{2+} levels were measured over time after disrupting the integrity of the Golgi with Brefeldin A (i.e., BFA). To verify the dispersal of the Golgi, 3T3 cells treated with BFA for 30 minutes were fixed with methanol and subsequently stained with antibodies targeting the Golgi (IFT20) and cilia (Arl13b). Treatment with 1.0μM BFA for 30 minutes was sufficient to fully disperse the Golgi (Figure 11B and 11C). To test whether dispersing the Golgi impacts cilia Ca^{2+}

in living cells, cilia Ca^{2+} levels were measured for 30 minutes after 30 minutes of incubation with of 1.0μM BFA. When individual cilia Ca^{2+} levels from individual cells were measured over 30 minutes in we found that cilia show a change in Ca^{2+} over time after BFA treatment. This response appeared to cluster into two groups, with one showing a greater increase in Ca^{2+}over time than the other (Figure 11D). The results from each individual cilium were averaged for both BFA treated cells and DMSO treated cells and showed that BFA treated cells show a greater change in Ca^{2+} after 30 minutes (Figure 11E). These data provide a starting point for future iterations of this experiment where imaging conditions will be optimized to limit photobleaching and keep cells under optimal temperature and CO_2 conditions. Although cilia Ca^{2+} levels exhibited substantial variability, these preliminary results suggest that Golgi integrity may impact steady state Ca^{2+} levels in cilia.

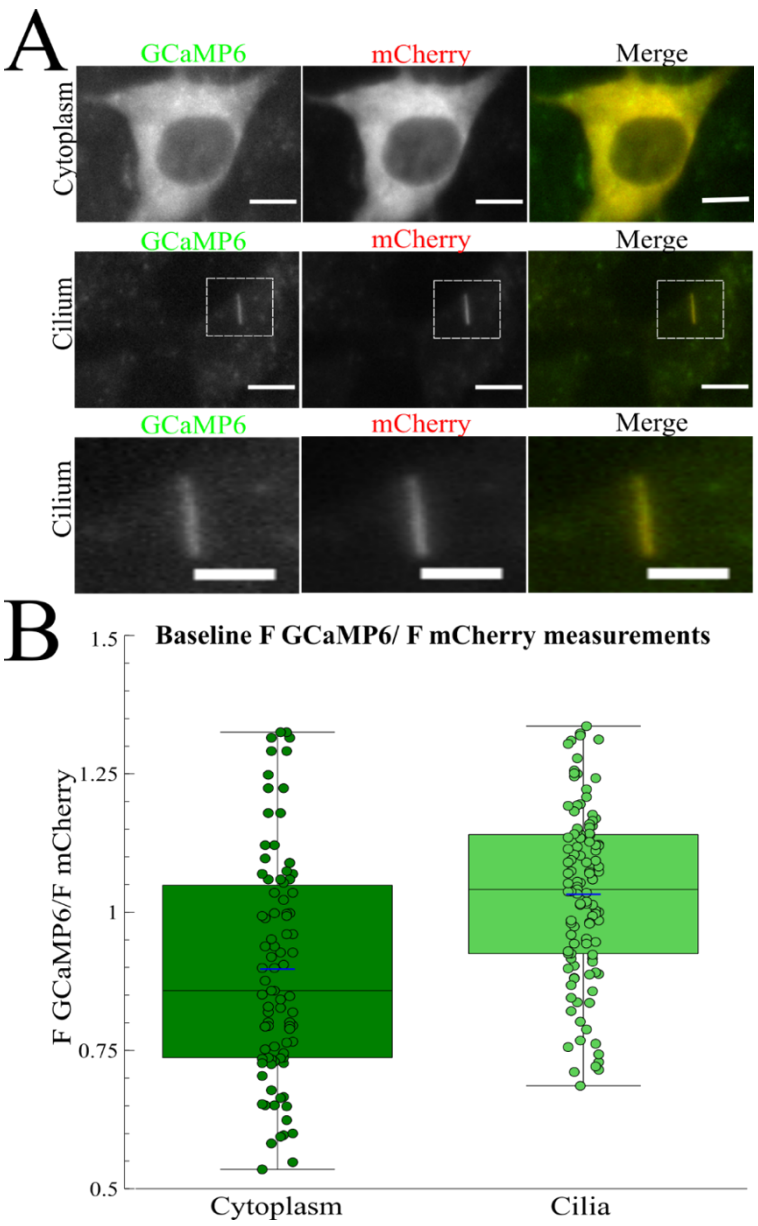

Figure 10. Establishing a tool for measuring Ca^{2+} *in vivo*
(A) NIH 3T3 cell expressing pcDNA5-FRT-TO-GCaMP6-mCherry a F GCaMP6/F mCherry ratio representative of the average for the cytoplasm (0.89). F GCaMP6/F mCherry ratio represents the fluorescence intensity of GCaMP6 divided by the fluorescence intensity of mCherry. The images below depict a cilium from a NIH 3T3 cell expressing pcDNA5-FRT-TO-GCaMP6-mCherry-Arl13b representative of the average F GCaMP6/F mCherry with a ratio representative of the average for cilia (1.05). Scale = 4 µm. **(B)** Distribution of F GCaMP6/F mCherry ratios among cells (i.e., cytoplasm) and cilia. Each point represents a single cell or cilium. Cytoplasm measurements in boxplot represent n = 90 from 24 different coverslips. Cilia measurements in boxplot represent n = 115 from 27 different coverslips. On average cilia have a greater ratio than the cytoplasm, consistent with previous studies on cilia Ca^{2+}.

Determining whether Ca^{2+} released from the Golgi can enter the cilium

After examining the effect of disrupting the integrity of the Golgi on cilia Ca^{2+}, the next objective was to investigate whether Ca^{2+} released from the Golgi is capable of entering cilia. To test this, the drugs histamine and thapsigargin were used to quickly stimulate the release of Ca^{2+} from the Golgi. Unavoidably, this drug combination can also stimulate the release of Ca^{2+} from the ER. Since the ER and the Golgi make membrane contacts with one another, the combined release of Ca^{2+} from the ER and Golgi was justified. The base of the cilium is often embedded within the Golgi, and the base of the cilium lacks a limiting membrane to selectively permit the entry of ions. Therefore, if cytoplasmic Ca^{2+} is elevated beyond cilia Ca^{2+} levels, the cilia Ca^{2+} concentration gradient should flip and thereby cause Ca^{2+} to freely diffuse from the cytoplasm into the ciliary compartment. In contrast, if Ca^{2+} originating from the Golgi cannot freely enter the cilium, then stimulating the Golgi with histamine and thapsigargin should not impact cilia Ca^{2+} levels.

To begin testing these predictions, NIH 3T3 cells were transfected with pcDNA5-FRT-TO-GCaMP6-mCherry (cytoplasmic Ca^{2+} sensor) and treated with 100μM histamine and thapsigargin. The temporal resolution of this experiment differs from that of the previous BFA experiment due to the short acting nature of histamine and thapsigargin. Imaging conditions and timing was optimized to limit photobleaching. Co-stimulation with histamine and thapsigargin produced a rapid increase in cytoplasmic Ca^{2+} (Figure 12C). At 90 sec. post-stimulation, the average fold-change in histamine/thapsigargin treated cytoplasmic Ca^{2+} was 1.589 with a standard deviation of 0.490.

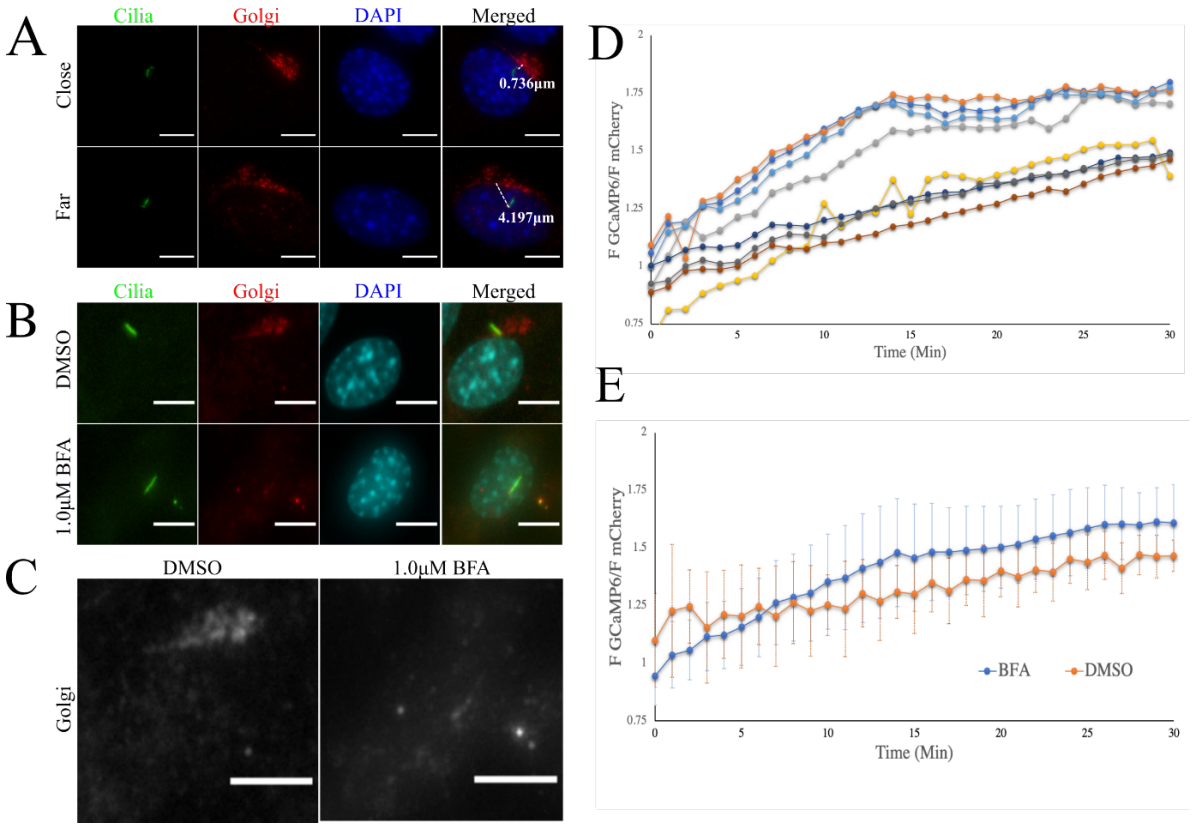

Figure 11. BFA causes dispersal of the Golgi

(A) NIH 3T3 cells with cilium localization close to the Golgi (less than 2µm) and a separate cilium with localization far from the Golgi (greater than 2µm). IFT20-mCherry reporter was used to visualize the Golgi (red) and primary cilia were stained with GT335 (green). DAPI was used to stain DNA shown in blue. Images courteously provided by Josh McNamara. Scale = 10µm. **(B)** The effects of BFA on NIH 3T3 cells. The Golgi is intact after the vehicle control (DMSO) was administered for 30 min. 1.0 µM BFA causes Golgi dispersal as depicted by IFT20 staining (red). Cilium is stained with IgG2a-Arl13b (green). Nucleus stained with DAPI (cyan). Scale = 4µm. **(C)** Zoomed in images from the Golgi response in panel B depicting change in localization of the Golgi in grey scale. Scale = 4µm. **(D)** Graph depicting change in F GCaMP6/ F mCherry after 1.0µM BFA over the course of 30 min. with image intervals of one min. **(E)** Graph showing F GCaMP6/F mCherry ratios of NIH 3T3 cells treated with BFA or DMSO vehicle control for 30 min. Each line represents the averaged response cilia from all cells treated with either BFA or DMSO.

(Figure 10F), while the average fold-change in DMSO treated cytoplasmic Ca^{2+} was 1.094 with a standard deviation of 0.122 (Supplemental 1A). These results indicate that co-stimulation with 100μM histamine and thapsigargin increases intracellular Ca^{2+} within 90 sec. of drug administration.

To determine whether Ca^{2+} from the Golgi rapidly enters cilia, NIH 3T3 cells were transfected with pcDNA5-FRT-TO-GCaMP6-mCherry-Arl13b (cilia sensor) and co-stimulated with histamine and thapsigargin. In contrast to the cytoplasm, where nearly all cells exhibited a rapid rise in Ca^{2+} upon co-stimulation, Ca^{2+} released from the Golgi did not always enter cilia (Figure 12E). While some cilia responded with an increase in Ca^{2+}, many did not (Figure 12D). In fact, some cilia experienced a decrease in Ca^{2+} levels after stimulation. The average fold-change in cilia Ca^{2+} after histamine and thapsigargin administration was 1.117 with a standard deviation of 0.163 for cells treated with histamine and thapsigargin (Figure 12G). Cilia administered the vehicle control consisting of DMSO and water showed an average fold change of 1.083 with a standard deviation of 0.079 (Supplemental 1B). These results suggest that Ca^{2+} from the Golgi does not always freely diffuse from the cytoplasm into the ciliary compartment.

One limitation of this experiment, however, is this experiment did not evaluate Ca^{2+} levels in the cilium and cytoplasm of the same cell simultaneously. This limitation makes it impossible to distinguish between two possible scenarios. Either some cilia did not respond because the corresponding cytoplasm responded weakly, or, alternatively, cilia did not respond because Ca^{2+} flux from intracellular stores into the ciliary compartment was not efficient. Distinguishing

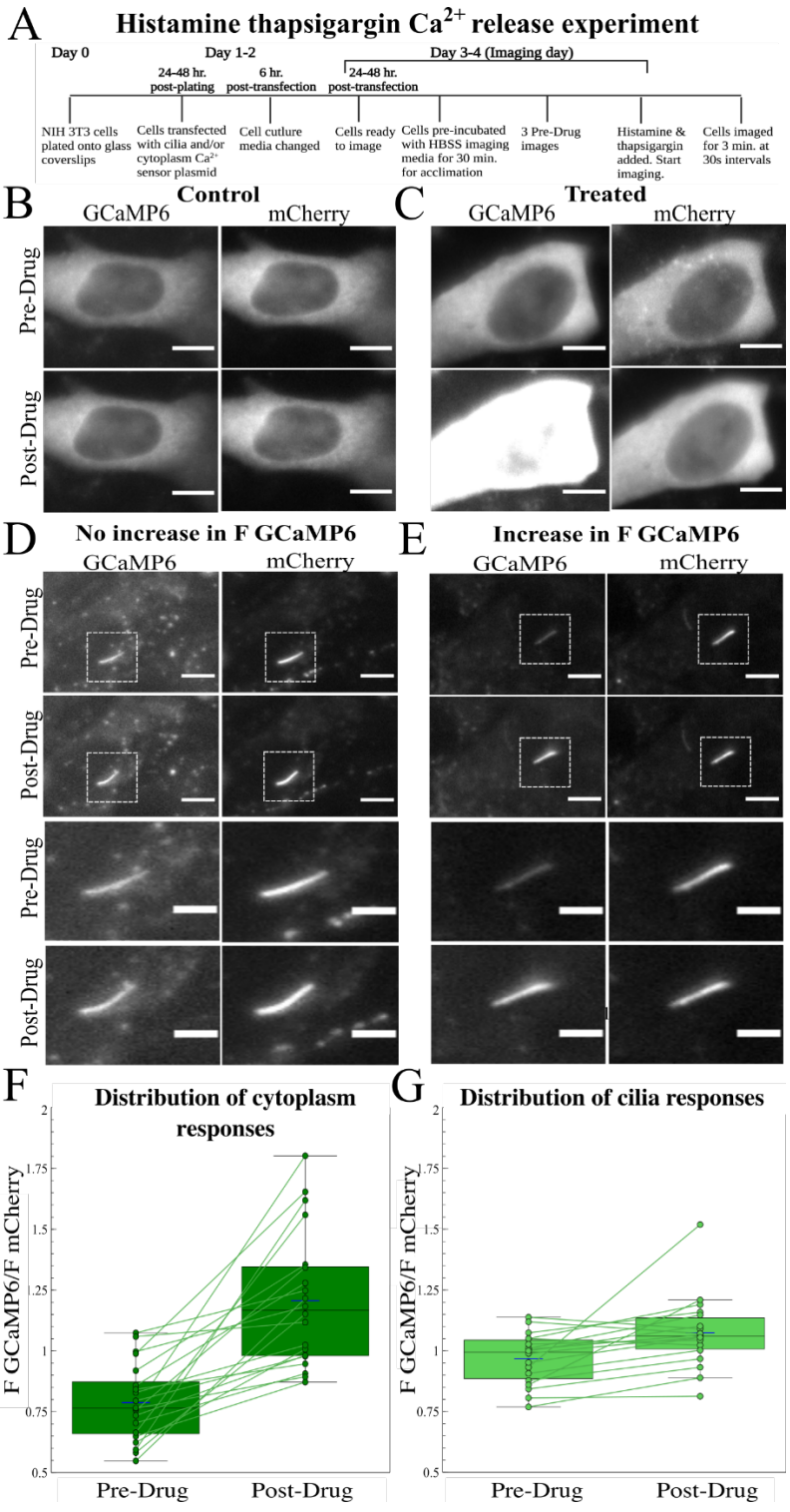

Figure 12. Cilia display a variable response to Ca^{2+} released from intracellular Ca^{2+}stores

(A) Experimental timeline for histamine thapsigargin co-stimulation experiment. NIH 3T3 cells were stimulated with histamine and thapsigargin following three pre-drug images. Once drug was administered, cells were imaged for 3 min. at 30 sec. intervals. **(B)** Cytoplasm response to water and DMSO control at 90 sec. Scale = 4µm**. (C)** Cytoplasm response to histamine and thapsigargin at 90 sec. Scale = 4µm**. (D)** Cilium from a NIH 3T3 cell that did not respond with an increase in F GCaMP6/ F mCherry ratio. Scale = 4µm for non-zoomed in images. For zoomed in images of cilium selected with white box, scale = 2µm **(E)** Cilium from a NIH 3T3 cell that did respond with an increase in F GCaMP6 intensity. Scale = 4µm for non-zoomed in images. For zoomed in images of cilium selected with white box, scale = 2µm**. (F)** Graphical representation of cytoplasm F GCaMP6/F mCherry ratio pre-drug vs. 90 sec. post-drug. **(G)** Graphical representation of cilia F GCaMP6/F mCherry ratios pre-drug vs. 90 sec. post-drug. Slope of the line between each timepoint indicates the magnitude of change between pre- and post- drug.

between these possibilities would provide insight into how cilia Ca^{2+} signaling is impacted by Ca^{2+} release from intracellular stores.

Monitoring cytoplasmic and ciliary Ca^{2+} simultaneously *in vivo*

To determine why cilia did not respond as robustly as the cytoplasm, NIH 3T3 cells were dual transfected for the visualization of both cytoplasmic Ca^{2+} and cilia Ca^{2+} simultaneously. Cells expressing both pcDNA5-FRT-TO-GCaMP6-mCherry-Arl13b (cilia localization) and pcDNA5-FRT-TO-GCaMP6-mCherry (cytoplasm localization) were treated with 100μM histamine and thapsigargin and both cytoplasmic Ca^{2+} levels and cilia Ca^{2+} levels were measured simultaneously. Results of dual transfected cells were consistent of that of the single transfected cells. By 90 seconds post 100μM histamine and thapsigargin, dual transfected NIH 3T3 cells experienced a sharp increase in cytoplasmic Ca^{2+} like that of single transfected cells. The average fold-change in cytoplasmic Ca^{2+} in dual transfected cells was 1.586 with a standard deviation of 0.482 for cells treated with histamine and thapsigargin (Figure 13E). Cells administered the vehicle control consisting of DMSO and water showed an average fold change of 1.049 with a standard deviation of 0.076 in the cytoplasm. Cilia treated with histamine and thapsigargin in dual transfected showed average fold-change of 1.124 with a standard deviation of 0.125 (Figure 13D). Cilia administered the vehicle control consisting of DMSO and water showed an average fold change of 1.051 with a standard deviation of 0.073 (Supplemental 2B). Together these results confirm the initial results from single transfected cell experiments. By conducting experiments using dual transfected cells we show that there are cells that experience a sharp increase in cytoplasmic Ca^{2+} that do not show free diffusion of Ca^{2+} into the cilium. Prior to the dual transfection experiment, it was not possible to infer whether cilia that showed little to no

response were associated with cells that responded to the histamine and thapsigargin administration with a rise in cytoplasmic Ca^{2+}.

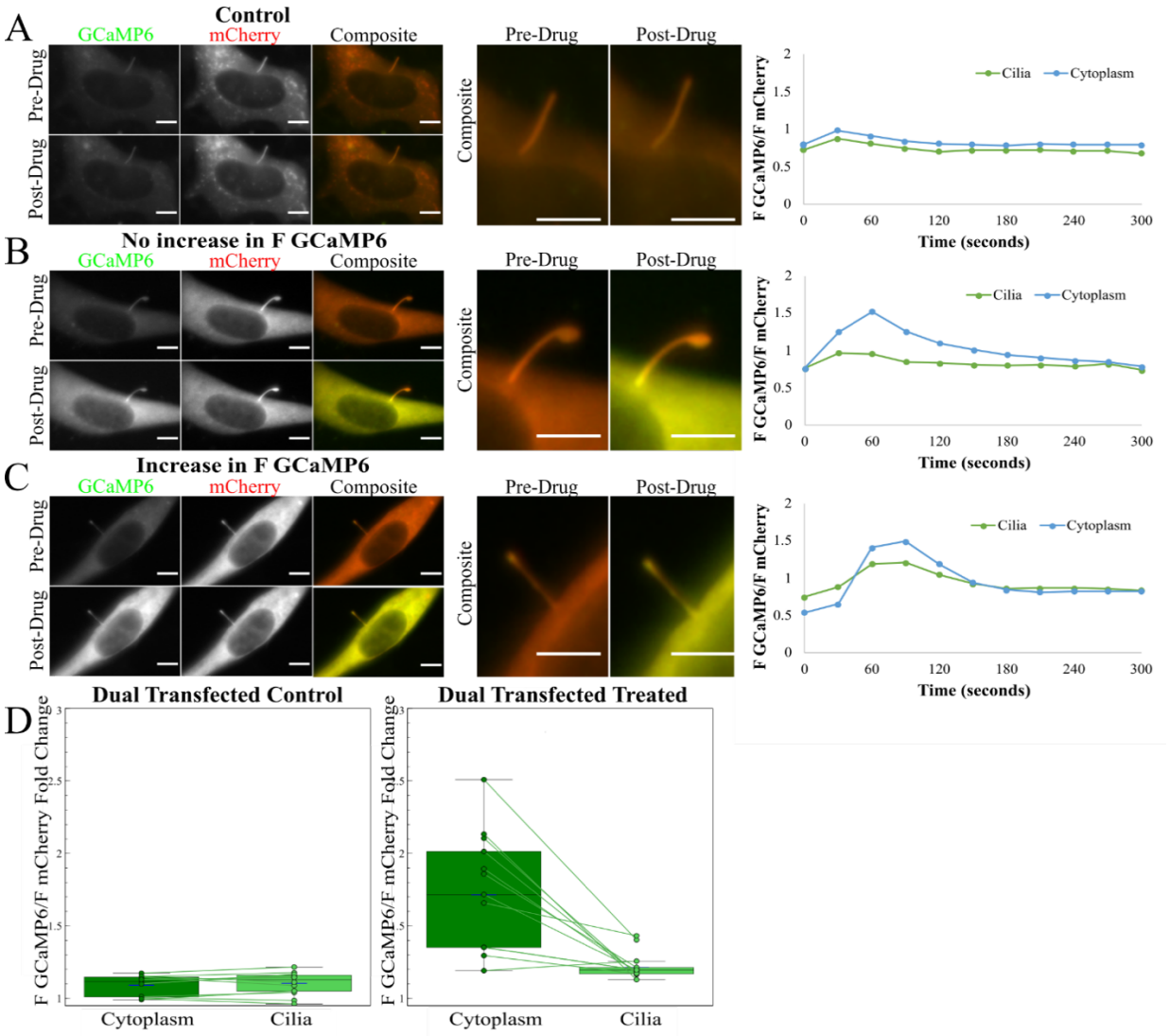

Figure 13. Analyzing both ciliary and cytoplasmic Ca^{2+} *in vivo* simultaneously
(A) NIH 3T3 cells dual transfected with both Ca^{2+} sensor plasmids (pcDNA5-FRT-TO-GCaMP6-mCherry and pcDNA5-FRT-TO-GCaMP6-mCherry-Arl13b) and graph of GCaMP6/mCherry ratio over time with DMSO/water treated cells. Scale = 4µm. **(B)** Images of NIH 3T3 cells dual transfected with both Ca^{2+} sensor plasmids (pcDNA5-FRT-TO-GCaMP6-mCherry and pcDNA5-FRT-TO-GCaMP6-mCherry-Arl13b) and graph of GCaMP6/mCherry ratio over time with histamine and thapsigargin treated cells. The no response cell shows little to no increase in F GCaMP6 intensity at the cilium, while there is a clear increase in F GCaMP6 in the cytoplasm. Scale = 4µm. **(C)** Images of NIH 3T3 cells dual transfected with both Ca^{2+} sensor plasmids (pcDNA5-FRT-TO-GCaMP6-mCherry and pcDNA5-FRT-TO-GCaMP6-mCherry-Arl13b) and graph of GCaMP6/mCherry ratio over time with histamine and thapsigargin treated cells. The response cell shows an increase in F GCaMP6 intensity at the cilium when stimulated with 100µM histamine and thapsigargin. Scale = 4µm. **(D)** Graphs depicting the ratio fold change in the cilium vs. the cytoplasm at 90 sec. post-drug. Fold change is measuring the change between the pre-drug F GCaMP6/F mCherry and F GCaMP6/F mCherry at 90 sec. post-drug. The line connecting the two points indicate that those two measurements are from the same single cell.

The fact that cilia are mechanically sensitive is well established. The mechanism by which the Ca^{2+} enters the cilium is not well understood. The membrane that surrounds the cilium (i.e., ciliary membrane) is enriched with Ca^{2+}-permeable channels, such as polycystin 2 (PC-2) and transient receptor potential cation channel subfamily V member 4 (TRPV4), by which Ca^{2+} is thought to pass through when cilia experience mechanical stress (Saternos et al., 2020; Sonkusare et al., 2012). Due to the mechanical sensitivity cilia display, the delivery of histamine and thapsigargin unavoidably creates a small rise in ciliary Ca^{2+}. This rise is short lived, and cilia go back to their resting Ca^{2+} state quickly after being disturbed. The peak response of histamine and thapsigargin occurs at approximately 90 seconds post drug administration, while the initial influx of Ca^{2+} due to the unavoidable fluid flow generated from delivering the drug occurs approximately 30 seconds post-drug delivery. To verify and account for any potential artifact, a mechanical stimulation experiment was conducted. Cilia were stimulated with mechanical force and analyzed over time for changes in Ca^{2+} (Figure 14A). Results from the mechanical stimulation experiment indicate that cilia experience a rise in Ca^{2+} approximately 30 seconds post-stimulation and recover by 60 seconds post-stimulation (Figure 14C). When dual transfected cells were mechanically stimulated, cilia experienced an average ratio increase of 0.128. Additionally, cilia stimulated with mechanical force show almost uniform increases in both time and magnitude as the cytoplasm (Figure 14C). These results show that mechanical stimulation causes a synchronized rise in both cilia and cytoplasmic Ca^{2+} and verifies that the timing of the histamine and thapsigargin response is due to the drug and not the delivery. While it is published that Ca^{2+} enters the cilium through Ca^{2+} channels that line the ciliary membrane, these results alone do not distinguish whether the mechanical stimulation increases ciliary Ca^{2+} from intracellular or extracellular origin. To ensure that the synchronized response was of

extracellular origin as literature would predict, a Ca^{2+} channel blocker experiment was conducted.

To confirm that the rapid rise in ciliary Ca^{2+} in response to mechanical stimulation was of extracellular origin, the Ca^{2+} channel blocker $LaCl_3$ was used to restrict the entry of extracellular Ca^{2+} through the ciliary and plasma membrane. As expected, dual transfected cells treated with 1mM $LaCl_3$ exhibited a decrease in both ciliary and cytoplasmic Ca^{2+} (Figure 15C). When dual transfected cells were mechanically stimulated in the presence of 1mM $LaCl_3$, cilia experienced an average ratio increase of 0.066 after mechanical stimulation events (Figure 16C). Collectively, the mechanical stimulation with and without $LaCl_3$ suggests that cilia Ca^{2+} levels are impacted by extracellular Ca^{2+} when mechanically stimulated which ultimately led to a decreased mechanical response from cilia and the cytoplasm. Additionally, these results distinguish the Ca^{2+}response caused from drug delivery from the response of the drug itself. Since the histamine and thapsigargin peak response occurs around 90 seconds, we can confidently conclude that the effect we see is due to the mechanism of action of each drug rather than the delivery itself.

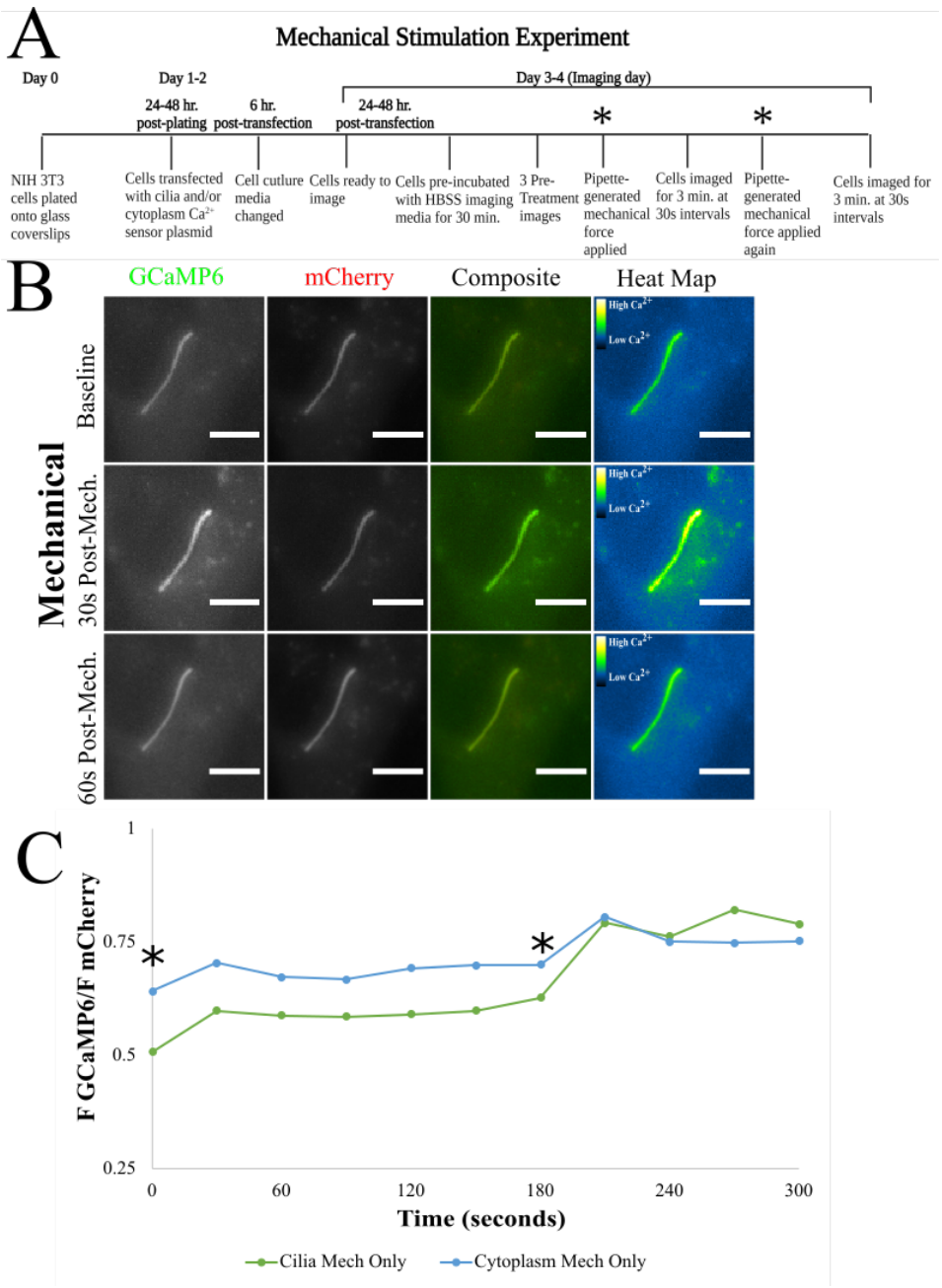

Figure 14. Mechanical stimulation causes an increase in cilia Ca^{2+}
(A) Experimental timeline for mechanical stimuli experiment with NIH 3T3 cells. Cells were stimulated with mechanical force following three pre-treatment (i.e., baseline) images. Cells were imaged for 3 min. at 30 sec. intervals. At 180 sec., a second mechanical stimuli was applied to cells and imaged for another 3 min. at 30 sec. intervals. **(B)** Images of a cilium from NIH 3T3 cells pre- and post- mechanical stimulation. Heat map corresponds to F GCaMP6 signal intensity. Images show an increase in F GCaMP6 after mechanical stimulation followed by a recovery within 30 sec. Scale = 4μm. **(C)** Graph showing the quantified effect of mechanical stimulation on a dual transfected cell. Mechanical stimulation applied at T=0 and T= 180 and indicated on graph and timeline with an asterisk.

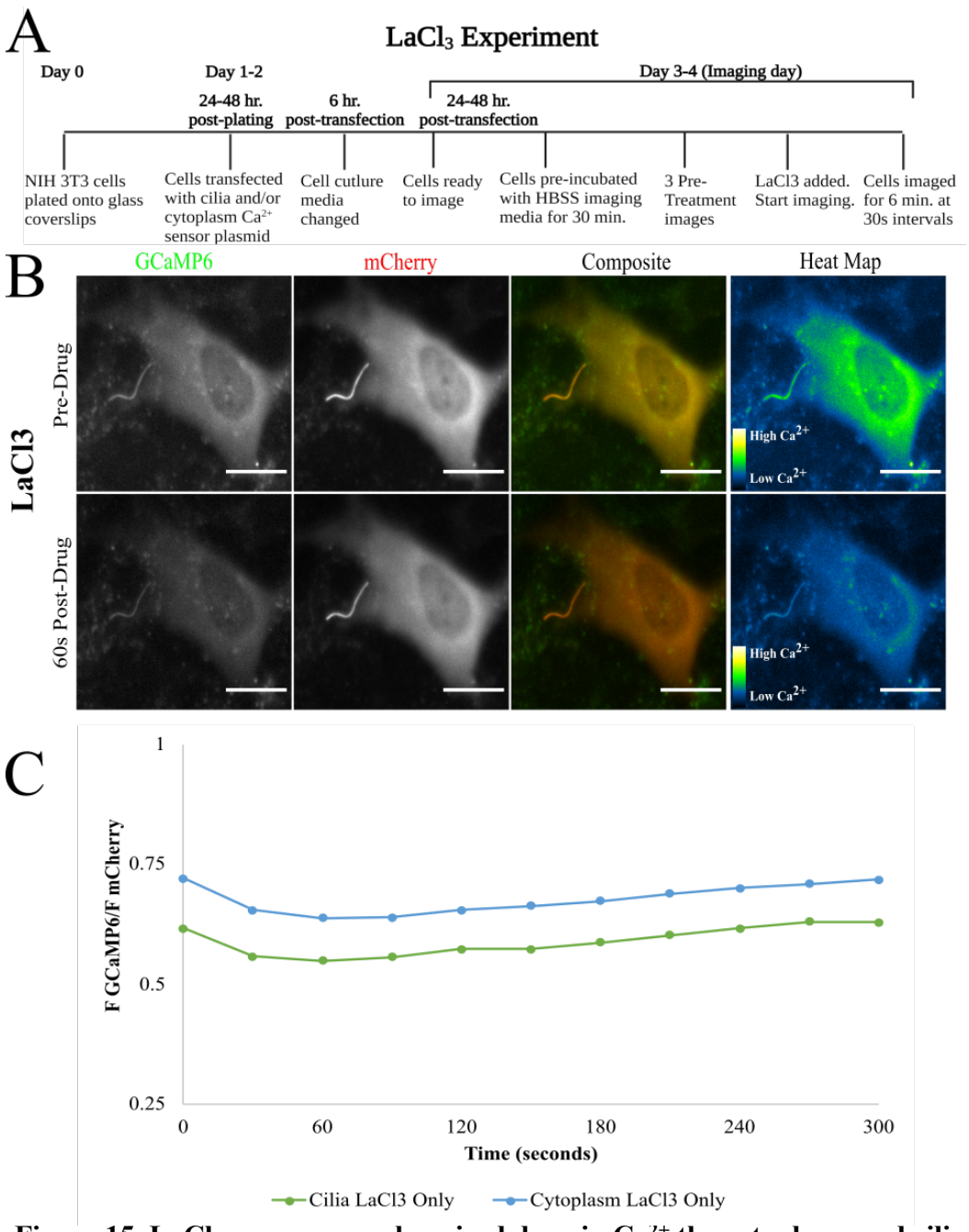

Figure 15. $LaCl_3$ causes a synchronized drop in Ca^{2+} the cytoplasm and cilium **(A)** Experimental timeline for $LaCl_3$ experiment with NIH 3T3 cells. Cells were administered 1mM $LaCl_3$ following three pre-treatment images. Cells were imaged for 6 min. at 30 sec. intervals. **(B)** Images of dual transfected NIH 3T3 cells pre- and post-$LaCl_3$ administration. Heat map corresponds to GCaMP6 signal intensity. Images show a decrease in GCaMP6/mCherry ratio in both the cilium and cytoplasm within 60 sec. Scale = 4μm. **(C)** Corresponding graph showing the quantified effect of $LaCl_3$ on the cilium and cytoplasm over 6 min.

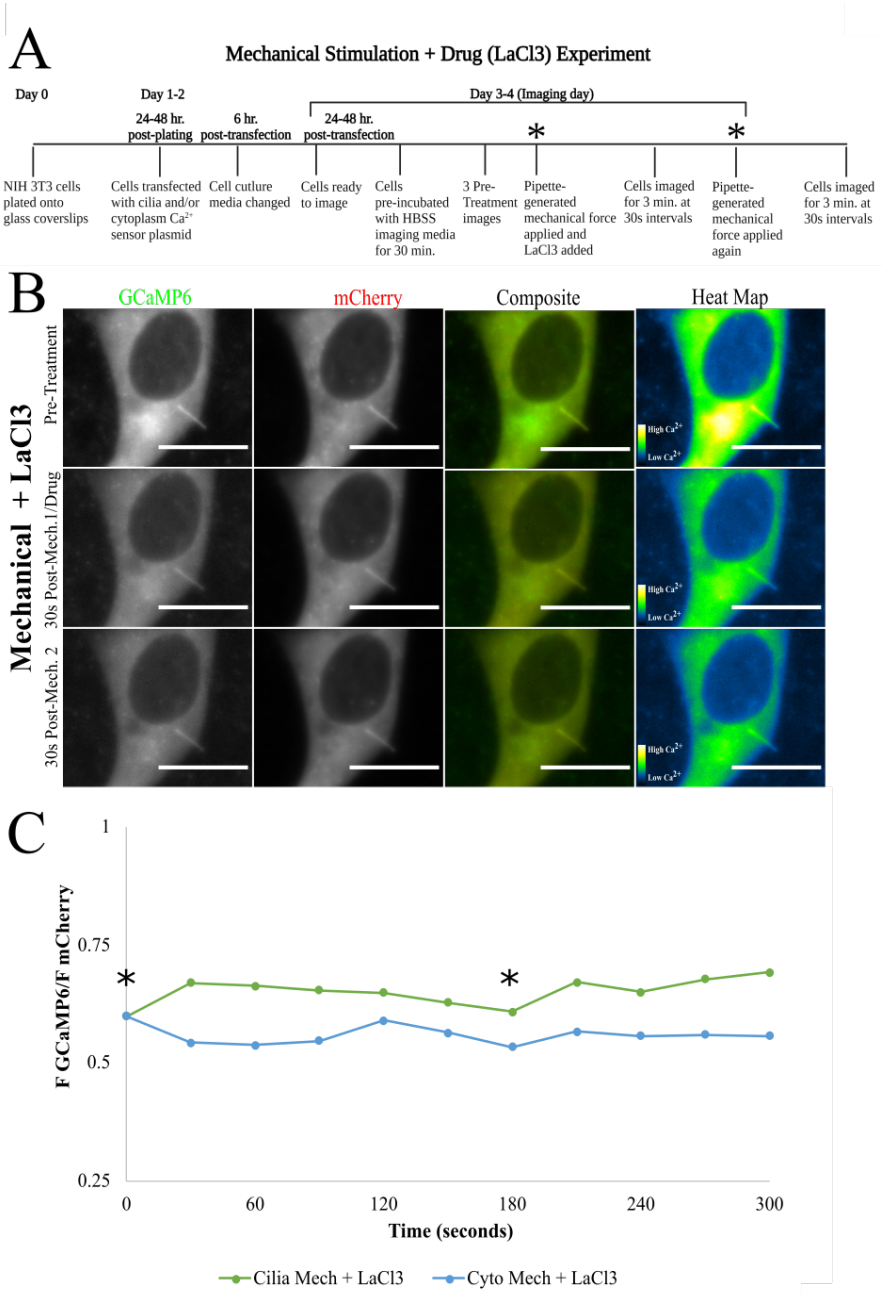

Figure 16. $LaCl_3$ decreases ciliary response to mechanical stimuli
(A) Experimental timeline for $LaCl_3$ and mechanical stimuli experiment with NIH 3T3 cells. Cells were administered 1mM $LaCl_3$ and stimulated with mechanical force following three pre-treatment images. Cells were imaged for 3 min. at 30 sec. intervals. At 180 sec., a second mechanical stimuli was applied to cells and imaged for another 3 min. at 30 sec. intervals. **(B)** Images of a dual transfected NIH 3T3 cells pre- and post- mechanical stimulation and LaCl3 administration. Heat map corresponds to F GCaMP6 signal intensity. Scale = 10µm. **(C)** Graph showing the quantified effect of mechanical stimulation on a dual transfected cell treated with $LaCl_3$. Both drug and stimuli applied at T=0s with mechanical stimuli repeated at T=180s, indicated by an asterisk on graph and experimental timeline.

cause consistent increases in ciliary Ca^{2+} levels, but mechanical stimulation did cause consistent increases in ciliary Ca^{2+}, these results suggest that ciliary Ca^{2+} response may be different based on the source of Ca^{2+}, intracellular or extracellular. Thus, differential mechanisms may exist to regulate Ca^{2+} entry into the ciliary compartment from inside the cell, a possible expansion of the current "outside-in" model.

These preliminary results suggest that cilia respond differently whether Ca^{2+} is coming from inside or outside of the cell. These results also show that not all cilia display the same response to sudden rises of intracellular Ca^{2+} as confirmed by dual transfection experiments monitoring cilia Ca^{2+} and cytoplasmic Ca^{2+} simultaneously. However, before these results can be interrupted broadly, the limitation of a low number of replicates must be considered. Many of the previous studies on cilia Ca^{2+} also contain a low number of replicates and much of this comes down to the biological limitations of doing these experiments (Delling et al., 2013; Delling et al., 2016). Cilia are often sparse in cultured cells and transfection experiments carry variable levels of transfection efficiency (Figure 17B). In dual transfected cells, measurable cells are very hard to come by as both expression and cilia positioning must be optimal (Figure 17C). For example, cilia that have overlap with the rest of the cell cannot be measured due to the inability to distinguish fluorescence between the cilium and rest of the cytoplasm (Figure 17D). These factors make measuring a large population of cilia difficult. One way to increase the population of measurable cilia is to generate a cell line capable of permanently expressing the required fluorescent reporters at stable levels.

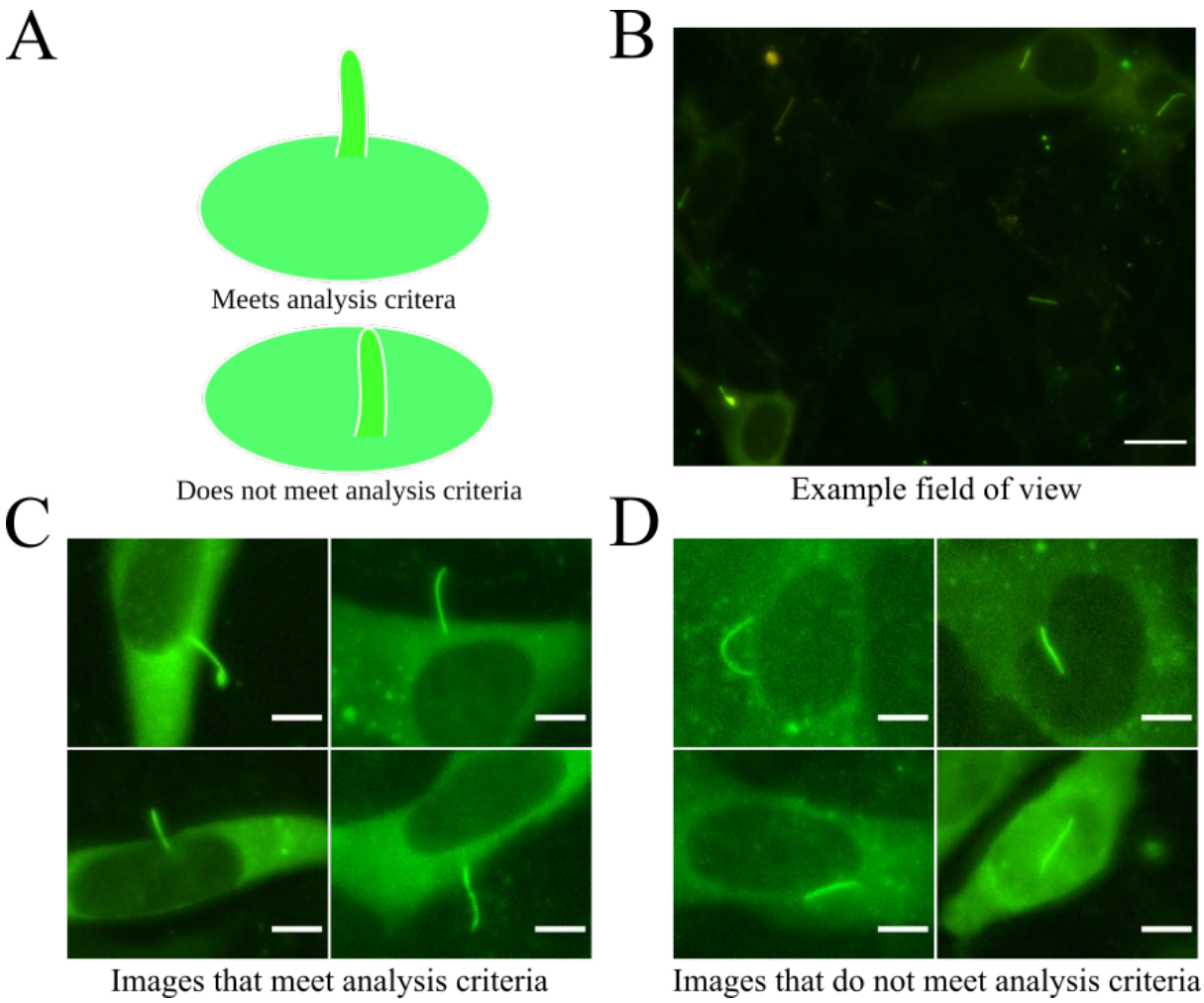

Figure 17. Criteria for ratiometric analysis of dual transfected cells
(A) Graphic displaying a simplified example of what cells can be analyzed. Cilia that overlap with the cell cannot be imaged due to the interference of fluorescence from the cytoplasm. **(B)** Example field of view from a dual transfected coverslip showing that there are very few cilia that can be analyzed despite many being visible. Scale = 10µm. **(C)** Examples of 3T3 cells expressing GCaMP6 that could be analyzed due to cilia not overlapping with the cell. Scale = 4µm. **(D)** Examples of 3T3 cells expressing GCaMP6 that could not be analyzed due to cilia overlapping with the cell. Scale = 4µm.

Establishing a stable cell line

The results described in previous sections relied on transient transfection experiments, which are laborious and problematic for generating experimental replicates. To overcome this obstacle, the last objective of this project was to engineer a stable cell line. The cell line was genetically engineered to express the GCaMP6-mCherry-Arl13b construct necessary to quantify cilia Ca^{2+} levels and a mammalian selection marker to select for cells that successfully integrated the plasmid. To create the cell line, a new plasmid was constructed by sub-cloning the neomycin antibiotic resistance gene from pH2b-emiRFP670 into pcDNA5-FRT-TO-GCaMP6-mCherry-Arl13b to form a new plasmid. Subcloning successfully led to the engineering of a plasmid for the GCaMP6-mCherry-Arl13b 3T3 cell line (Figure 18).

A kill curve experiment using the vector plasmid was conducted to establish the optimal dose of the analogue of neomycin, G418, for cell selection (Figure 19A). Cells were plated at various G418 concentrations and observed over 8 days. 600μg/ml was selected as the optimal dose. At 600μg/ml, the cells were predicted to live for a period of 3-4 days, enough time to keep cells healthy long enough for plasmid incorporation but not allow non-transfected cells to survive.

To create the cell line, cells were plated at ~30% confluency and transfected one day post-plating. As expected, non-transfected cells not treated with G418 (i.e., - drug) remained healthy with many mitotic cells (Figure 19B), while non-transfected cells cultured in 600μg/ml G418 (i.e., + drug) were dead by 96 hours (Figure 19B). In contrast, although transfected cells treated with G418 experienced cell death, some cells survived the first 96 hours (Figure 19B). After 12 days of selection using G418 and regular passaging, polyclonal cell populations expressing GCaMP6-mCherry-Arl13b were identified through live cell imaging of a subpopulation of cells

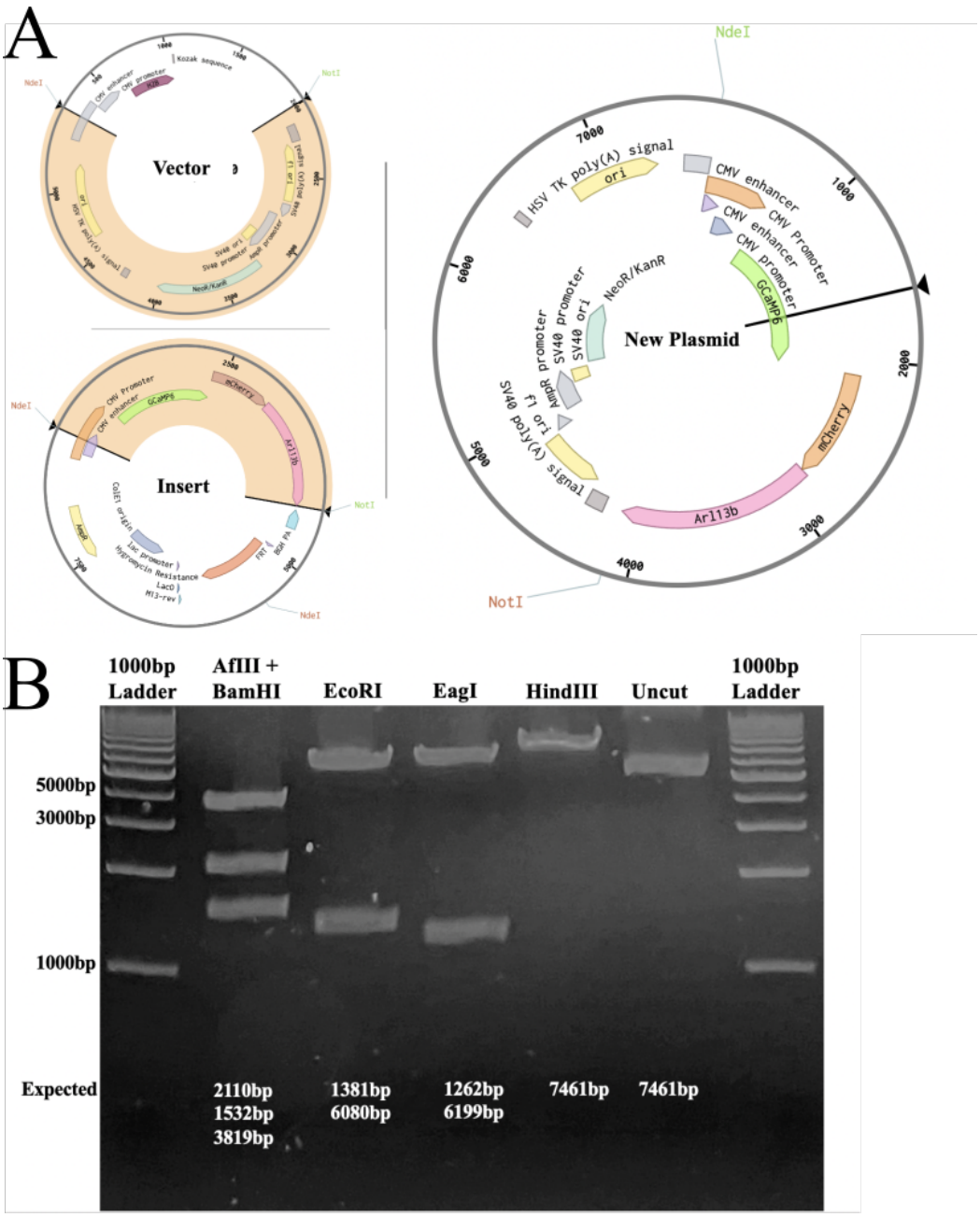

Figure 18. New construct made to express neomycin resistance for cell selection

Plasmid map of the plasmid made specifically for engineering a stable cell line expressing GCaMP6-mCherry-Arl13b. This plasmid was generated from subcloning techniques utilizing PCR to remove isolate from pcDNA5-FRT-TO-GCaMP6-Arl13b and pH2b-emiRFP670 and ligate them to form the new construct. pH2b-emiRFP670 was used to remove a fragment conferring neomycin resistance so that it could be included to provide a mammalian selection marker for stable cell line selection. **(B)** Confirmation of correct plasmid through restriction enzyme digests. 0.7% agarose gel ran by Josh McNamara.

plated onto coverslips (Figure 19C). G418 concentration was dropped from 600ug/ml to 400ug/ml for the remaining selection to lower stress on the cells. To confirm that these surviving cells expressed the cilia calcium reporter, coverslips containing the polyclonal cell population were fixed and stained for cilia (Figure 19D), which indicated that the stable transfection efficiency was ~5%. To convert the polyclonal cell population into monoclonal populations via limiting dilution. In total, 160 clones were screened to select for colonies of cells that originate from one single cell, resulting in a limited number of stable clones that expressed the cilia calcium reporter at reasonable levels (i.e., monoclonal cell population; Figure 19C). Of these candidate clones, clone originally positioned in A6 of the 96-well plate displayed the best expression and became the primary monoclonal cell line produced from this process (Figure 19E). This clonal cell line is currently being used to increase the replicates for the previous BFA experiments using the Leica Stellaris8 confocal microscope with an environmental control chamber. An additional benefit that comes with the cell line is the fact that cilia will express the Ca^{2+} sensor at stable levels consistently, which also makes it easier to conduct experiments where one might want to use live-cell stain or transfection for the visualization of other subcellular components.

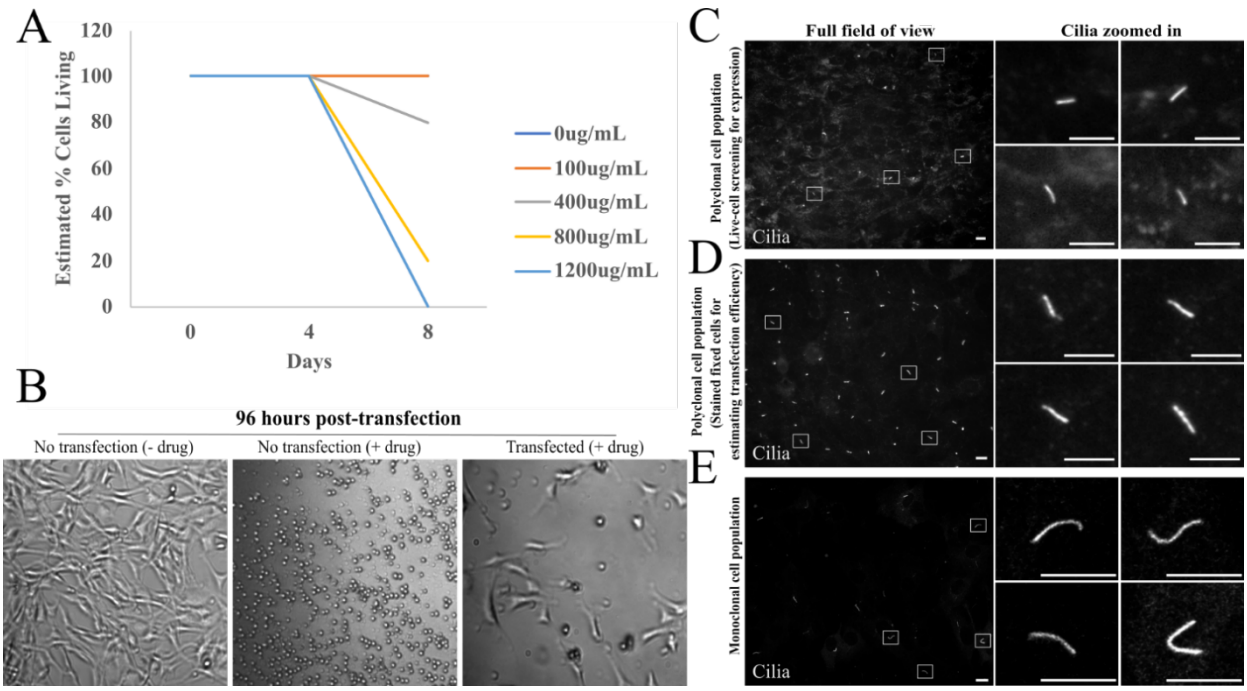

Figure 19. Monoclonal cell line selection

(A) Kill curve of G418 on NIH 3T3 cells. An intermediate between 400µg/mL and 800µg/mL dose was chosen. Cells transfected with the new construct (Figure 15) were selected using 600µg/mL G418 in DMEM + 10% calf serum. **(B)** Cells that were not transfected with the plasmid conferring G418 resistance were plated as a control. One subset of no transfection control cells was cultured without the presence of G418 (i.e.., - drug) and the other was cultured in the presence of G418. Cells cultured in 600µg/mL were killed off by 96 hours. Cells that were transfected with the plasmid and cultured in drug displayed cells expressing G418 resistance displayed cell death, but many cells remained. **(C)** Transfected + drug cells at 12 days post transfection showing a polyclonal population. Scale = 10µm. **(D)** Cells that were imaged at day 12 fixed and stained for cilia (Arl13b). The number of cilia stained was compared to the number of cilia found during live-cell imaging to estimate transfection efficiency. Transfection efficiency was approximated to be 5%. Scale = 10µm. **(E)** Cells expressing GCaMP6-mCherry-Al13b isolated from a single cell. Scale = 10µm.

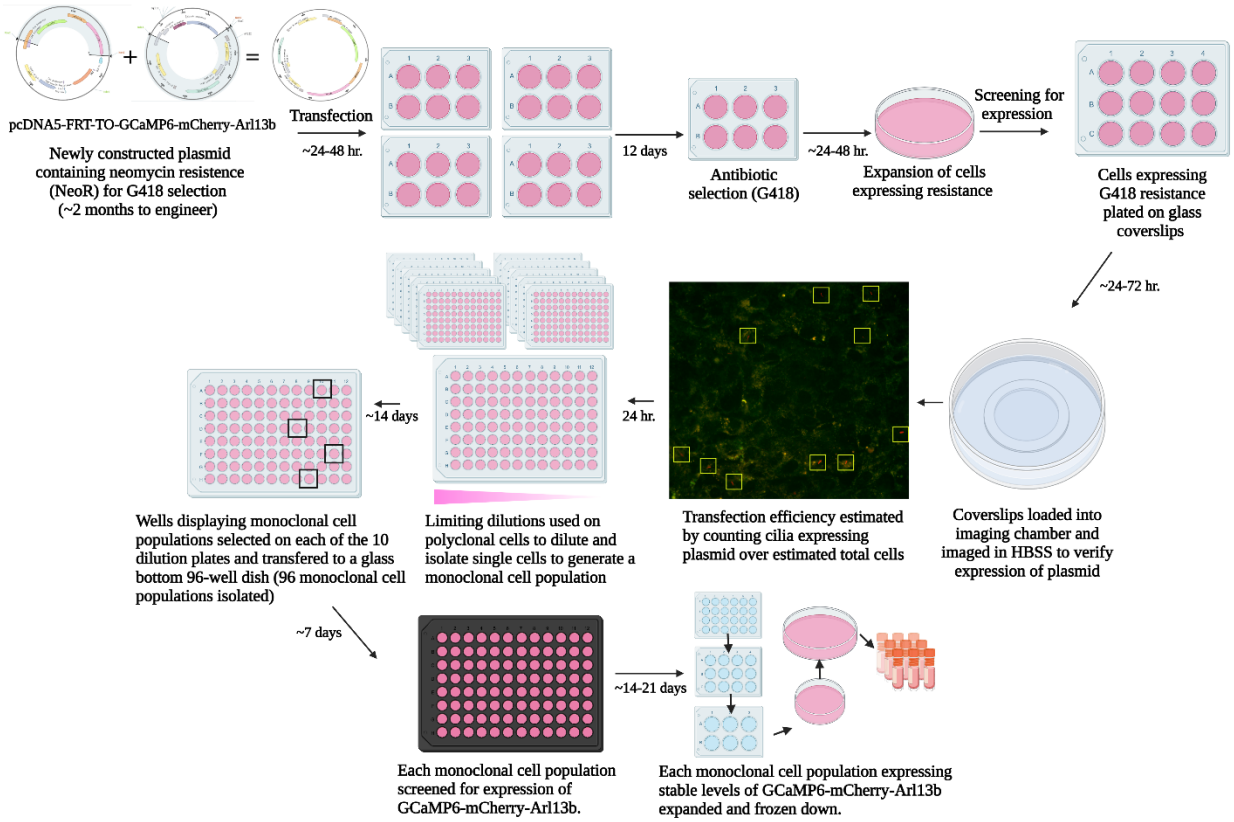

Figure 20. Schematic of monoclonal cell line workflow
Schematic depicting the process of generating and selecting a monoclonal cell line. The final product was a monoclonal cell line of NIH 3T3 cells expressing GCaMP6-mCherry-Arl13b, and cells were expanded and frozen down for future use in the lab.

Discussion

Through this work, we sought to understand the mechanisms that govern ciliary Ca^{2+} homeostasis. Specifically, we wanted to determine whether the Golgi is capable of influencing cilia Ca^{2+} levels. Three approaches were deployed. First, the proximity between the base of the cilium and the Golgi was analyzed. Secondly, cilia Ca^{2+} levels were examined after disrupting the structural integrity of the Golgi. Finally, the effects of Ca^{2+} released from the Golgi was assessed by measuring cilia Ca^{2+} in response to histamine thapsigargin co-stimulation. Previous work established a model of ciliary Ca^{2+} suggesting that cilia maintain a distinct Ca^{2+} environment with up to seven-fold higher Ca^{2+} than the cytoplasm. This "outside-in" model suggests that Ca^{2+} levels are maintained through Ca^{2+} channels that line the ciliary membrane through a favorable influx/efflux ratio. Additionally, this model suggests that Ca^{2+} may go from the cilium to the cytoplasm through simple diffusion based on the existing concentration gradient between the cilium (~700nM) and the cytoplasm (~100nM). This model fails to account for the variable proximity of cilia to Ca^{2+}-buffering organelles such as the Golgi or ER, which can raise the local Ca^{2+} concentration beyond 700 nM. (Mohr et al., 1987; Ma and Beaven 2009). Since Ca^{2+}-buffering organelles can form contact points to transfer Ca^{2+}, this raises the question as to whether these membranes bound Ca^{2+}-buffering organelles facilitate Ca^{2+} transfer at non-membrane-bound organelle such as the cilium.

On average, 8% of NIH 3T3 cells have cilia with a separation distance of more than 2μm from the Golgi. Meaning, in 92% of NIH 3T3 cells cilia reside very close to the Golgi, and many are even be embedded within the Golgi (Josh McNamara, personal comm.). It is unclear how this spatial coupling of the cilium and the Golgi impacts Ca^{2+} levels in cilia. To examine the potential

contribution of Ca^{2+} from the Golgi to cilia, the structural integrity of the Golgi was disrupted with BFA. Results show that cilia treated with 1.0μM BFA showed higher levels of Ca^{2+} when compared to cilia treated with DMSO after 30 minutes (Figure 11E). Interestingly, when individual cilia are compared to one another after treatment with BFA, there appears to be two groups in terms of the magnitude of the rise in Ca^{2+} (Figure 11D). Perhaps one explanation of this grouping could be the spatial coupling of the cilium and the Golgi. Some cilia are farther from the Golgi which could decrease the magnitude of Ca^{2+} contribution from the Golgi. In terms of the overall rise in Ca^{2+} measured in cilia, one possibility is that cilia Ca^{2+} increases when the Golgi is disrupted due to the Ca^{2+} stored within the Golgi mobilizing as the Golgi dissociates, leading to the release into the surrounding environment. When the cilium is embedded within the Golgi, the Golgi can no longer selectively buffer Ca^{2+}. Instead, Ca^{2+} contents of the Golgi leak out into the cell and potentially enter the ciliary compartment. This could suggest that the Golgi impacts both the influx and efflux of Ca^{2+} from the ciliary compartment. To expand on this dataset, this experiment is being repeated and optimized to include a climate-controlled imaging chamber and the ability to image in the normal culturing media (DMEM). However, these preliminary results suggest that the Golgi may be impacting cilia Ca^{2+} homeostasis.

Next, experiments were conducted in effort to flip the concentration gradient between the cilium and the cytoplasm via strong Ca^{2+} release from Ca^{2+} -buffering storage organelles. If cilia calcium homeostasis is largely controlled by free diffusion of Ca^{2+}, then Ca^{2+} should be able to freely diffuse from the higher concentration in the cytoplasm to the lower concentration in the cilium (Figure 10B). Through a combination of techniques in quantitative microscopy and molecular biology, we tested this model. When cells were stimulated to release Ca^{2+} from the ER

and Golgi, cilia displayed a non-homogeneous response (Figure 12G). These results suggest that even when the concentration gradient between the cilium and the cytoplasm is reversed, free diffusion does not always occur. If free diffusion were the only process governing Ca^{2+} compartmentalization within cilia, we would expect to see an influx of Ca^{2+} similar to the cytoplasm in both magnitude and timing. Additionally, cilia with lower initial Ca^{2+} levels than the cytoplasm did not experience free diffusion of Ca^{2+} after intracellular Ca^{2+} release even when the gradient established by Delling et al. 2013 was flipped at the start of the experiment (Figure 13C).

In contrast to the intracellular Ca^{2+} release experiments, when cells were stimulated with mechanical force, the cilium and cytoplasm showed very similar responses (i.e., lockstep response; Figure 21D). When cilia are mechanically stimulated, the influx of Ca^{2+} occurs synchronously in both cilia and the cytoplasm upon the initial mechanical stimulation and the second stimulation at 180 seconds (Figure 14C). Due to this we believe this influx of Ca^{2+} when mechanical force is applied is due to the entry of extracellular Ca^{2+}. To test this, cells were mechanically stimulated in the presence of the Ca^{2+} channel blocker, $LaCl_3$. We found that cells treated with $LaCl_3$ display less of an influx in Ca^{2+} in both the cytoplasm and the cilium. At both stimulation events T=0 and T=180, cilia and cytoplasm Ca^{2+} increased less than cells not treated with $LaCl_3$. One caveat to this interpretation is that $LaCl_3$ blocks calcium from channels lining the plasma and ciliary membrane, and efficacy and timing of complete restriction of Ca^{2+} may be difficult in cilia given that the ciliary membrane has an estimated 50-fold more Ca^{2+} channels than the rest of the plasma membrane (Delling et al., 2013). Nonetheless, our data support a new

model whereby cilia exhibit a non-uniform response to intracellular calcium release but a rather homogenous response to extracellular calcium entry.

In addition to the non-uniform response seen when Ca^{2+} was released from intracellular Ca^{2+} stores, we also found that often cilia do not have a higher F GCaMP6/F mCherry ratio than the cytoplasm. We saw this in dual transfected cells when both cytoplasmic Ca^{2+} and ciliary Ca^{2+} could be measured simultaneously (Figure 13D). This observation further strengthens the idea that there is more governing the maintenance of Ca^{2+} in the ciliary compartment than diffusion. This also raises the question as to what factors may influence such a difference in steady-state Ca^{2+} observations. One factor may be that this is the first study to quantify Ca^{2+} in cilia of mouse fibroblast cells (i.e., NIH 3T3). The current model of ciliary Ca^{2+} was established using a different a different cell line, human retinal pigment epithelial cells (i.e., hTERT RPE). There is no evidence to support that cilia maintain Ca^{2+} differentially in cell types, but due to the different functions of cell types and lack of data on cilia Ca^{2+} among different cell lines, this cannot be ruled out.

The biological relevance of these experiments can be connected to recent work examining the role of Ca^{2+} transients in cilia and the cytoplasm during the process of L-R asymmetry body plan development. Ca^{2+} transients in the cytoplasm of mouse crown cells are required to establish L-R asymmetry during development. Mizuno and colleagues recently found that there are essential components to generate L-R asymmetry in cytoplasmic Ca^{2+} transients in crown cells. They found that nodal flow generated from motile cilia, extracellular Ca^{2+} entry through PKD2 channels, and intracellular Ca^{2+} entry by IP3 activation are all required for L-R asymmetry

establishment (Mizuno et al., 2020). Interestingly, this implies that fluid flow generated by motile cilia at the embryonic node generates specific Ca^{2+} conditions in conjunction with extracellular Ca^{2+} entering through PKD channels that surround the ciliary and plasma membrane. Additionally, intracellular Ca^{2+} originating from the ER and Golgi from the activation of the IP3 pathway were essential for cilia and cytoplasm Ca^{2+} transients. When parvalbumin was overexpressed in cilia of crown cells, they found that loss of ciliary and cytoplasmic Ca^{2+} transients was sufficient to disrupt L-R asymmetry. These results indicate that Ca^{2+} binding proteins within cilia contribute to Ca^{2+} modulation in both the ciliary compartment and cytoplasm (Mizuno et al., 2020).

Together, the experiments in this work, along with published data, suggest an expansion of the current model of ciliary calcium regulation by which Ca^{2+} may be modulated by the presence of Ca^{2+}-binding proteins located at the base cilium or within the cilium serving as gatekeepers, chelating Ca^{2+} from freely diffusing into the ciliary compartment in the presence of steep Ca^{2+} gradients. With the data surrounding basal body proximity to prominent Ca^{2+}-buffering organelles, this provokes an interesting question as to that spatial coupling may impact ciliary Ca^{2+} levels through the selectivity of evolutionarily conserved Ca^{2+}-binding proteins. Preliminary experiments evaluating ciliary Ca^{2+} in response to mechanical force and the extracellular Ca^{2+} blocker $LaCl_3$, suggest that cilia can experience immediate Ca^{2+} entry of Ca^{2+} of extracellular origin, while cilia experience little or no Ca^{2+} entry of Ca^{2+} released from the Golgi and ER. Mizuno et al. 2020 show that mechanical stimuli sensed by cilia from crown cells initiates a critical increase in cilia Ca^{2+} required for L-R asymmetry in early embryonic development. Additionally, the IP3 pathway controlling Ca^{2+} release from the ER and Golgi has been

implicated in this process, suggesting that Ca^{2+} originating from within the cell serves a role in modulating L-R asymmetry. As for Ca^{2+} from outside of the cell, PKD channels that line the ciliary and plasma membrane were shown to be essential for L-R asymmetry establishment as well, suggesting that Ca^{2+} originating from outside of the cell is also critical. Together, this suggests that both intracellular Ca^{2+} and extracellular Ca^{2+} contribute to ciliary Ca^{2+} homeostasis, further highlighting the importance of uncovering the underlying mechanisms.

This work aimed to illuminate some of those mechanisms by examining the contribution of Ca^{2+} from both within the cell and outside of the cell. Collectively we found that the "outside-in" model can be applied when Ca^{2+} originates from outside of the cell, however, this model contradicts how cilia respond when Ca^{2+} originates from inside of the cell (Figure 21). This work should encourage investigators to continue testing these models and to evaluate the possibility that other Ca^{2+} buffering organelles contribute to ciliary Ca^{2+}. Knock-down or overexpression experiments targeting specific Ca^{2+}-binding proteins at the basal body may also be useful in finalizing a "inside-out" model of ciliary Ca^{2+}.

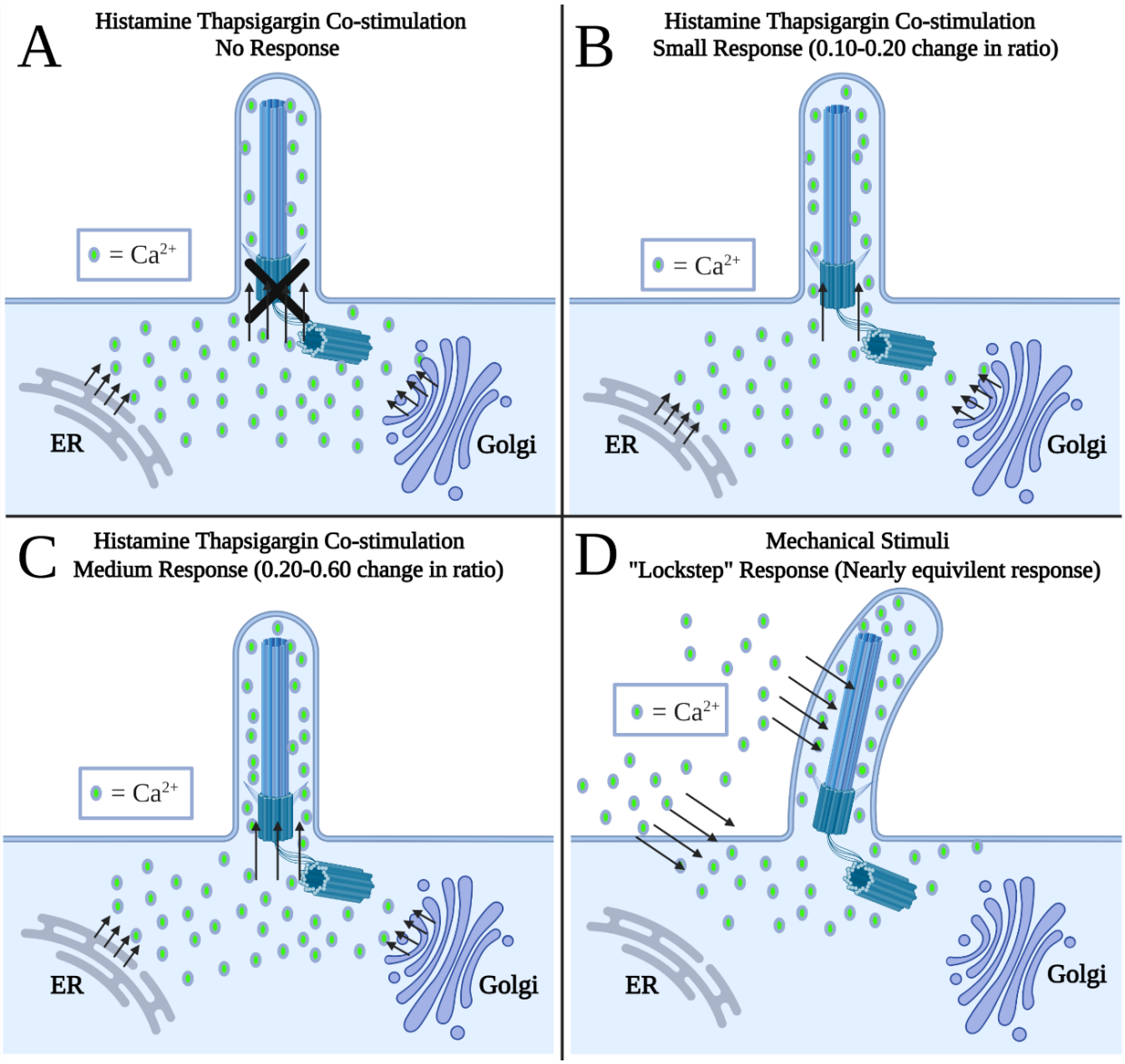

Figure 21. Summary of cilia responses and hypothesized source
(A) Depiction of cilia displaying no response to histamine and thapsigargin induced intracellular Ca^{2+} release defined by no change in F GCaMP6/F mCherry ratio. **(B)** Depiction of cilia displaying a small response to histamine and thapsigargin induced intracellular Ca^{2+} release defined by an increase in F GCaMP6/F mCherry ratio of 0.10-0.20. **(C)** Depiction of cilia displaying a medium response to histamine and thapsigargin induced intracellular Ca^{2+} release defined by an increase in F GCaMP6/F mCherry of 0.20-0.60. **(D)** Depiction of cilia displaying a lockstep response to mechanical stimuli defined by defined a nearly equivalent increase in F GCaMP6/F mCherry in both the cilium and cytoplasm. This response is predicted to be mostly of extracellular origin.

Literature Cited

Aguilar-Maldonado, B.; Gómez-Viquez, L.; García, L.; Del Angel, R. M.; Arias-Montaño, J. A.; Guerrero-Hernández, A. Histamine Potentiates IP3-Mediated Ca2+ Release via ThapsigarginSensitive Ca2+ Pumps. *Cellular Signalling* 2003, *15* (7), 689–697.

Ahluwalia, J. P.; Topp, J. D.; Weirather, K.; Zimmerman, M.; Stamnes, M. A Role for Calcium in Stabilizing Transport Vesicle Coats *. *Journal of Biological Chemistry* 2001, *276* (36), 34148–34155.

Akerboom, Jasper, Tsai-Wen Chen, Trevor J. Wardill, Lin Tian, Jonathan S. Marvin, Sevinç Mutlu, Nicole Carreras Calderón, et al. "Optimization of a GCaMP Calcium Indicator for Neural Activity Imaging." *Journal of Neuroscience* 32, no. 40 (October 3, 2012): 13819–40.

Bagur, R.; Hajnóczky, G. Intracellular Ca2+ Sensing: Role in Calcium Homeostasis and Signaling. *Mol Cell* 2017, *66* (6), 780–788.

Bisgrove, Brent W., and H. Joseph Yost. "The Roles of Cilia in Developmental Disorders and Disease." *Development* 133, no. 21 (November 1, 2006): 4131–43.

Blacque, O. E.; Reardon, M. J.; Li, C.; McCarthy, J.; Mahjoub, M. R.; Ansley, S. J.; Badano, J. L.; Mah, A. K.; Beales, P. L.; Davidson, W. S.; Johnsen, R. C.; Audeh, M.; Plasterk, R. H. A.; Baillie, D. L.; Katsanis, N.; Quarmby, L. M.; Wicks, S. R.; Leroux, M. R. Loss of C. Elegans BBS-7 and BBS-8 Protein Function Results in Cilia Defects and Compromised Intraflagellar Transport. *Genes Dev* 2004, *18* (13), 1630–1642.

Blum, Martin, and Philipp Vick. "Left–Right Asymmetry: Cilia and Calcium Revisited." *Current Biology* 25, no. 5 (March 2015): R205–7.

Carafoli, E. Calcium Signaling: A Tale for All Seasons. Proc Natl Acad Sci U S A 2002, 99 (3), 1115–1122.

Carafoli, E.; Krebs, J. Why Calcium? How Calcium Became the Best Communicator *. *Journal of Biological Chemistry* 2016, *291* (40), 20849–20857.

Carvalho-Santos, Z.; Azimzadeh, J.; Pereira-Leal, José. B.; Bettencourt-Dias, M. Tracing the Origins of Centrioles, Cilia, and Flagella. *Journal of Cell Biology* 2011, *194* (2), 165–175.

Chardin, P.; McCormick, F. Brefeldin A: The Advantage of Being Uncompetitive. *Cell* 1999, *97* (2), 153–155

Chazin, W. J. Relating Form and Function of EF-Hand Calcium Binding Proteins. *Acc Chem Res* 2011, *44* (3), 171–179.

Chen, Z.; Truong, T. M.; Ai, H. Illuminating Brain Activities with Fluorescent Protein-Based Biosensors. *Chemosensors* 2017, *5* (4), 32.

Collier, Daniel M., Nuria Villalba, Adrian Sackheim, Adrian D. Bonev, Zachary D. Miller, Jesse S. Moore, Bo Shui, et al. "Extracellular Histones Induce Calcium Signals in the Endothelium of Resistance-Sized Mesenteric Arteries and Cause Loss of Endothelium-Dependent Dilation." *American Journal of Physiology. Heart and Circulatory Physiology* 316, no. 6 (June 1, 2019): H1309–22.

Craft, J. M.; Harris, J. A.; Hyman, S.; Kner, P.; Lechtreck, K. F. Tubulin Transport by IFT Is Upregulated during Ciliary Growth by a Cilium-Autonomous Mechanism. *J Cell Biol* 2015, *208* (2), 223–237.

Dawe, H. R.; Farr, H.; Gull, K. Centriole/Basal Body Morphogenesis and Migration during Ciliogenesis in Animal Cells. *Journal of Cell Science* 2007, *120* (1), 7–15.

Delling, M., A. A. Indzhykulian, X. Liu, Y. Li, T. Xie, D. P. Corey, and D. E. Clapham. "Primary Cilia Are Not Calcium-Responsive Mechanosensors." Nature 531, no. 7596 (March 2016): 656–60.

Delling, Markus, Paul G. DeCaen, Julia F. Doerner, Sebastien Febvay, and David E. Clapham. "Primary Cilia Are Specialized Calcium Signaling Organelles." Nature 504, no. 7479 (December 12, 2013): 311–14.

Dombeck, D. A.; Harvey, C. D.; Tian, L.; Looger, L. L.; Tank, D. W. Functional Imaging of Hippocampal Place Cells at Cellular Resolution during Virtual Navigation. *Nat Neurosci* 2010, *13* (11), 1433–1440.

Engel, B. D.; Ishikawa, H.; Wemmer, K. A.; Geimer, S.; Wakabayashi, K.; Hirono, M.; Craige, B.; Pazour, G. J.; Witman, G. B.; Kamiya, R.; Marshall, W. F. The Role of Retrograde Intraflagellar Transport in Flagellar Assembly, Maintenance, and Function. *J Cell Biol* 2012, *199* (1), 151–167.

Ezzati, Mohammad, Ovrang Djahanbakhch, Sara Arian, and Bruce R. Carr. "Tubal Transport of Gametes and Embryos: A Review of Physiology and Pathophysiology." *Journal of Assisted Reproduction and Genetics* 31, no. 10 (October 2014): 1337–47.

Follit, John A., Richard A. Tuft, Kevin E. Fogarty, and Gregory J. Pazour. "The Intraflagellar Transport Protein IFT20 Is Associated with the Golgi Complex and Is Required for Cilia Assembly." *Molecular Biology of the Cell* 17, no. 9 (September 2006): 3781–92.

Fujiwara, T.; Oda, K.; Yokota, S.; Takatsuki, A.; Ikehara, Y. Brefeldin A Causes Disassembly of the Golgi Complex and Accumulation of Secretory Proteins in the Endoplasmic Reticulum. *J Biol Chem* 1988, *263* (34), 18545–18552.

Galati, D. F.; Mitchell, B. J.; Pearson, C. G. Subdistal Appendages Stabilize the Ups and Downs of Ciliary Life. *Developmental Cell* 2016, *39* (4), 387–389.

Grimes, D. T.; Burdine, R. D. Left-Right Patterning: Breaking Symmetry to Asymmetric Morphogenesis. *Trends Genet* 2017, *33* (9), 616–628.

Haupt, Amanda, Tanya Grancharova, Joy Arakaki, Margaret A. Fuqua, Brock Roberts, and Ruwanthi N. Gunawardane. "Endogenous Protein Tagging in Human Induced Pluripotent Stem Cells Using CRISPR/Cas9." Journal of Visualized Experiments: JoVE, no. 138 (25 2018).

Higginbotham, H.; Eom, T.-Y.; Mariani, L. E.; Bachleda, A.; Gukassyan, V.; Hirt, J.; Cusack, C.; Lai, C.; Caspary, T.; Anton, E. S. Arl13b in Primary Cilia Regulates the Migration and Placement of Interneurons in the Developing Cerebral Cortex. *Dev Cell* 2012, *23* (5), 925–938.

Hildebrandt, Friedhelm, Thomas Benzing, and Nicholas Katsanis. "Ciliopathies." *The New England Journal of Medicine* 364, no. 16 (April 21, 2011): 1533–43.

Inaba, K. Calcium Sensors of Ciliary Outer Arm Dynein: Functions and Phylogenetic Considerations for Eukaryotic Evolution. *Cilia* 2015, *4* (1), 6.

Ishikawa, H.; Marshall, W. F. Ciliogenesis: Building the Cell's Antenna. *Nat Rev Mol Cell Biol* 2011, *12* (4), 222–234.

Jaffe, Lionel F. "Fast Calcium Waves." *Cell Calcium* 48, no. 2–3 (September 2010): 102–13.

Jaskulska, A.; Janecka, A. E.; Gach-Janczak, K. Thapsigargin—From Traditional Medicine to Anticancer Drug. *Int J Mol Sci* 2020, *22* (1), 4.

Kaufman, Randal J., and Jyoti D. Malhotra. "Calcium Trafficking Integrates Endoplasmic Reticulum Function with Mitochondrial Bioenergetics." *Biochimica et Biophysica Acta* 1843, no. 10 (October 2014): 2233–39.

Kozminski, K. G.; Johnson, K. A.; Forscher, P.; Rosenbaum, J. L. A Motility in the Eukaryotic Flagellum Unrelated to Flagellar Beating. *Proc Natl Acad Sci U S A* 1993, *90* (12), 5519–5523.

Laoukili, J., E. Perret, S. Middendorp, O. Houcine, C. Guennou, F. Marano, M. Bornens, and F. Tournier. "Differential Expression and Cellular Distribution of Centrin Isoforms during Human Ciliated Cell Differentiation in Vitro." *Journal of Cell Science* 113 (Pt 8) (April 2000): 1355–64.

Lechtreck, K. F. IFT-Cargo Interactions and Protein Transport in Cilia. *Trends Biochem Sci* 2015, *40* (12), 765–778.

Lechtreck, K. F.; Brown, J. M.; Sampaio, J. L.; Craft, J. M.; Shevchenko, A.; Evans, J. E.; Witman, G. B. Cycling of the Signaling Protein Phospholipase D through Cilia Requires the BBSome Only for the Export Phase. *J Cell Biol* 2013, *201* (2), 249–261.

Lee, Soyeon, and Kyung-Tai Min. "The Interface Between ER and Mitochondria: Molecular Compositions and Functions." *Molecules and Cells* 41, no. 12 (December 31, 2018): 1000–1007.

Lewit-Bentley, A.; Réty, S. EF-Hand Calcium-Binding Proteins. *Current Opinion in Structural Biology* 2000, *10* (6), 637–643.

Lodh, Sukanya, Junji Yano, Megan S. Valentine, and Judith L. Van Houten. "Voltage-Gated Calcium Channels of Paramecium Cilia." *The Journal of Experimental Biology* 219, no. 19 (October 1, 2016): 3028–38. Heizmann, Claus W., and Willi Hunzlker. "Intracellular Calcium-Binding Proteins: More Sites than Insights." *Trends in Biochemical Sciences* 16 (January 1, 1991): 98–103.

Ma, H.-T.; Beaven, M. A. Regulation of Ca2+ Signaling with Particular Focus on Mast Cells. *Crit Rev Immunol* 2009, *29* (2), 155–186.

Marshall, Wallace F., and Christopher Kintner. "Cilia Orientation and the Fluid Mechanics of Development." *Current Opinion in Cell Biology* 20, no. 1 (February 2008): 48–52.

Mesmin, B.; Kovacs, D.; D'Angelo, G. Lipid Exchange and Signaling at ER-Golgi Contact Sites. *Curr Opin Cell Biol* 2019, *57*, 8–15.

Micaroni, Massimo. "Calcium around the Golgi Apparatus: Implications for Intracellular Membrane Trafficking." *Advances in Experimental Medicine and Biology* 740 (2012): 439–60.

Mitchell, D. R. Evolution of Cilia. *Cold Spring Harb Perspect Biol* 2017, *9* (1), a028290.

Mitchison, Hannah M., and Enza Maria Valente. "Motile and Non-Motile Cilia in Human Pathology: From Function to Phenotypes." *The Journal of Pathology* 241, no. 2 (2017): 294–309.

Mizuno, K.; Shiozawa, K.; Katoh, T. A.; Minegishi, K.; Ide, T.; Ikawa, Y.; Nishimura, H.; Takaoka, K.; Itabashi, T.; Iwane, A. H.; Nakai, J.; Shiratori, H.; Hamada, H. Role of Ca2+ Transients at the Node of the Mouse Embryo in Breaking of Left-Right Symmetry. *Science Advances* 2020, *6* (30), eaba1195.

Mlinar, B.; Enyeart, J. J. Block of Current through T-Type Calcium Channels by Trivalent Metal Cations and Nickel in Neural Rat and Human Cells. *J Physiol* 1993, *469*, 639–652.

Mohr, F. C.; Fewtrell, C. Depolarization of Rat Basophilic Leukemia Cells Inhibits Calcium Uptake and Exocytosis. *J Cell Biol* 1987, *104* (3), 783–792.

Moore, Bryn S., Ann N. Stepanchick, Paul H. Tewson, Cassandra M. Hartle, Jin Zhang, Anne Marie Quinn, Thomas E. Hughes, and Tooraj Mirshahi. "Cilia Have High CAMP Levels

That Are Inhibited by Sonic Hedgehog-Regulated Calcium Dynamics." *Proceedings of the National Academy of Sciences* 113, no. 46 (November 15, 2016): 13069–74.
Morshedian, Ala, and Gordon L. Fain. "The Evolution of Rod Photoreceptors." *Philosophical Transactions of the Royal Society B: Biological Sciences* 372, no. 1717 (April 5, 2017).
Nachshen, D. A. Selectivity of the Ca Binding Site in Synaptosome Ca Channels. Inhibition of Ca Influx by Multivalent Metal Cations. *J Gen Physiol* 1984, *83* (6), 941–967.
Nachury, M. V.; Loktev, A. V.; Zhang, Q.; Westlake, C. J.; Peränen, J.; Merdes, A.; Slusarski, D. C.; Scheller, R. H.; Bazan, J. F.; Sheffield, V. C.; Jackson, P. K. A Core Complex of BBS Proteins Cooperates with the GTPase Rab8 to Promote Ciliary Membrane Biogenesis. *Cell* 2007, *129* (6), 1201–1213.
Nakai, J.; Ohkura, M.; Imoto, K. A High Signal-to-Noise Ca(2+) Probe Composed of a Single Green Fluorescent Protein. *Nat Biotechnol* 2001, *19* (2), 137–141.
Nilsson, Dan-e. "Eye Evolution and Its Functional Basis." *Visual Neuroscience* 30, no. 1–2 (March 2013): 5–20.
Nockolds, C. E.; Kretsinger, R. H.; Coffee, C. J.; Bradshaw, R. A. Structure of a Calcium-Binding Carp Myogen. *Proceedings of the National Academy of Sciences* 1972, *69* (3), 581–584.
Nonaka, S.; Shiratori, H.; Saijoh, Y.; Hamada, H. Determination of Left–Right Patterning of the Mouse Embryo by Artificial Nodal Flow. *Nature* 2002, *418* (6893), 96–99. https://doi.org/10.1038/nature00849.
Nonaka, Shigenori, Satoko Yoshiba, Daisuke Watanabe, Shingo Ikeuchi, Tomonobu Goto, Wallace F Marshall, and Hiroshi Hamada. "De Novo Formation of Left–Right Asymmetry by Posterior Tilt of Nodal Cilia." *PLoS Biology* 3, no. 8 (August 2005).
Norris, D. P.; Jackson, P. K. Calcium Contradictions in Cilia. *Nature* 2016, *531* (7596), 582–583.
Okada, Y.; Nonaka, S.; Tanaka, Y.; Saijoh, Y.; Hamada, H.; Hirokawa, N. Abnormal Nodal Flow Precedes Situs Inversus in Iv and Inv Mice. *Molecular Cell* 1999, *4* (4), 459–468. https://doi.org/10.1016/S1097-2765(00)80197-5.
Ott, Carolyn, and Jennifer Lippincott-Schwartz. "Visualization of Live Primary Cilia Dynamics Using Fluorescence Microscopy." *Current Protocols in Cell Biology / Editorial Board, Juan S. Bonifacino ... [et Al.]* 0 4 (December 2012): Unit-4.26.
Pala, Rajasekharreddy, Nedaa Alomari, and Surya M. Nauli. "Primary Cilium-Dependent Signaling Mechanisms." *International Journal of Molecular Sciences* 18, no. 11 (October 28, 2017).
Pinton, Paolo, Tullio Pozzan, and Rosario Rizzuto. "The Golgi Apparatus Is an Inositol 1,4,5-Trisphosphate-Sensitive Ca2+ Store, with Functional Properties Distinct from Those of the Endoplasmic Reticulum." *The EMBO Journal* 17, no. 18 (September 15, 1998): 5298–5308.
Ravi, Bhavya, Layla M. Nassar, Richard J. Kopchock, Pravat Dhakal, Michael Scheetz, and Kevin M. Collins. "Ratiometric Calcium Imaging of Individual Neurons in Behaving Caenorhabditis Elegans." *Journal of Visualized Experiments: JoVE*, no. 132 (07 2018).
Reiter, Jeremy F., and Michel R. Leroux. "Genes and Molecular Pathways Underpinning Ciliopathies." Nature Reviews. Molecular Cell Biology 18, no. 9 (September 2017): 533–47.
Rieusset, J. The Role of Endoplasmic Reticulum-Mitochondria Contact Sites in the Control of Glucose Homeostasis: An Update. *Cell Death Dis* 2018, *9* (3), 388.

Saternos, H.; Ley, S.; AbouAlaiwi, W. Primary Cilia and Calcium Signaling Interactions. *Int J Mol Sci* 2020, *21* (19), 7109.
Satir, Peter, Thomas Heuser, and Winfield S. Sale. "A Structural Basis for How Motile Cilia Beat." *Bioscience* 64, no. 12 (December 1, 2014): 1073–83.
Sharifi Tabar, M.; Hesaraki, M.; Esfandiari, F.; Sahraneshin Samani, F.; Vakilian, H.; Baharvand, H. Evaluating Electroporation and Lipofectamine Approaches for Transient and Stable Transgene Expressions in Human Fibroblasts and Embryonic Stem Cells. *Cell J* 2015, *17* (3), 438–450.
Shaw, D. K.; Gunther, D.; Jurynec, M. J.; Chagovetz, A. A.; Ritchie, E.; Grunwald, D. J. Intracellular Calcium Mobilization Is Required for Sonic Hedgehog Signaling. *Developmental cell* 2018, *45* (4), 512.
Sigg, M. A.; Menchen, T.; Lee, C.; Johnson, J.; Jungnickel, M. K.; Choksi, S. P.; Garcia, G.; Busengdal, H.; Dougherty, G.; Pennekamp, P.; Werner, C.; Rentzsch, F.; Florman, H. M.; Krogan, N.; Wallingford, J. B.; Omran, H.; Reiter, J. F. Evolutionary Proteomics Uncovers Ancient Associations of Cilia with Signaling Pathways. *Dev Cell* 2017, *43* (6), 744-762.e11.
Sonkusare, S. K.; Bonev, A. D.; Ledoux, J.; Liedtke, W.; Kotlikoff, M. I.; Heppner, T. J.; Hill-Eubanks, D. C.; Nelson, M. T. Elementary Ca2+ Signals Through Endothelial TRPV4 Channels Regulate Vascular Function. *Science* 2012, *336* (6081), 597–601.
Szymanska, K.; Johnson, C. A. The Transition Zone: An Essential Functional Compartment of Cilia. *Cilia* 2012, *1* (1), 10.
Taillon, B. E.; Adler, S. A.; Suhan, J. P.; Jarvik, J. W. Mutational Analysis of Centrin: An EF-Hand Protein Associated with Three Distinct Contractile Fibers in the Basal Body Apparatus of Chlamydomonas. *Journal of Cell Biology* 1992, *119* (6), 1613–1624.
Tian, L.; Hires, S. A.; Mao, T.; Huber, D.; Chiappe, M. E.; Chalasani, S. H.; Petreanu, L.; Akerboom, J.; McKinney, S. A.; Schreiter, E. R.; Bargmann, C. I.; Jayaraman, V.; Svoboda, K.; Looger, L. L. Imaging Neural Activity in Worms, Flies and Mice with Improved GCaMP Calcium Indicators. *Nat Methods* 2009, *6* (12), 875–881. .
Tsien, R. W.; Hess, P.; McCleskey, E. W.; Rosenberg, R. L. CALCIUM CHANNELS: Mechanisms of Selectivity, Permeation, and Block. *Annu. Rev. Biophys. Biophys. Chem.* 1987, *16* (1), 265–290.
Verkhratsky, A.; Parpura, V. Calcium Signalling and Calcium Channels: Evolution and General Principles. *Eur J Pharmacol* 2014, *0*, 1–3.
Wang, Q.; Shui, B.; Kotlikoff, M. I.; Sondermann, H. Structural Basis for Calcium Sensing by GCaMP2. *Structure* 2008, *16* (12), 1817–1827.
Wictome, M.; Henderson, I.; Lee, A. G.; East, J. M. Mechanism of Inhibition of the Calcium Pump of Sarcoplasmic Reticulum by Thapsigargin. *Biochem J* 1992, *283* (Pt 2), 525–529.
Williams, C. L.; McIntyre, J. C.; Norris, S. R.; Jenkins, P. M.; Zhang, L.; Pei, Q.; Verhey, K.; Martens, J. R. Direct Evidence for BBSome-Associated Intraflagellar Transport Reveals Distinct Properties of Native Mammalian Cilia. *Nat Commun* 2014, *5*, 5813.
Yang, Zhaokang., Hannah M. Kirton, David A. MacDougall, John P. Boyle, James Deuchars, Brenda Frater, Sreenivasan Ponnambalam, et al. "The Golgi Apparatus Is a Functionally Distinct Ca2+ Store Regulated by PKA and Epac Branches of the B1-Adrenergic Signaling Pathway." *Science Signaling* 8, no. 398 (October 13, 2015).
Yoshiba, S.; Shiratori, H.; Kuo, I. Y.; Kawasumi, A.; Shinohara, K.; Nonaka, S.; Asai, Y.; Sasaki, G.; Belo, J. A.; Sasaki, H.; Nakai, J.; Dworniczak, B.; Ehrlich, B. E.; Pennekamp,

P.; Hamada, H. Cilia at the Node of Mouse Embryos Sense Fluid Flow for Left-Right Determination via Pkd2. *Science* 2012, *338* (6104), 226–231.

Supplemental Material

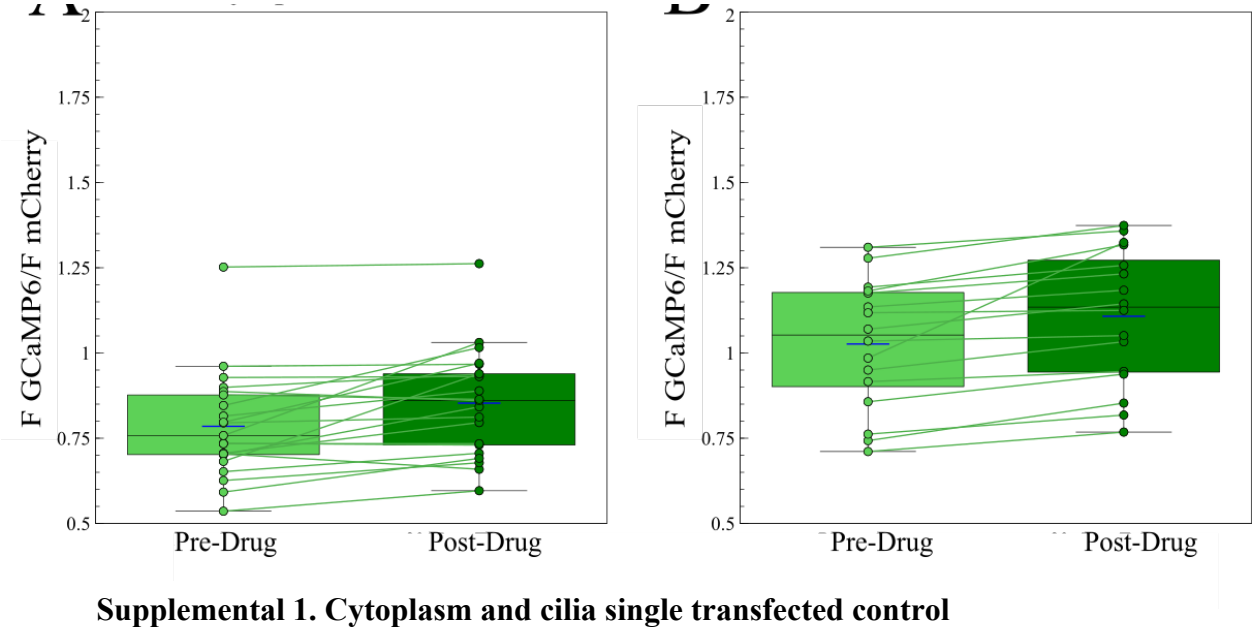

Supplemental 1. Cytoplasm and cilia single transfected control
Graphical representation of cytoplasm or cilia GCaMP/mCherry ratio pre-treatment (i.e., baseline) vs. 90 seconds post-treatment. Slope of the line between each timepoint indicates the magnitude of change between pre and post administration of the DMSO/water vehicle control.

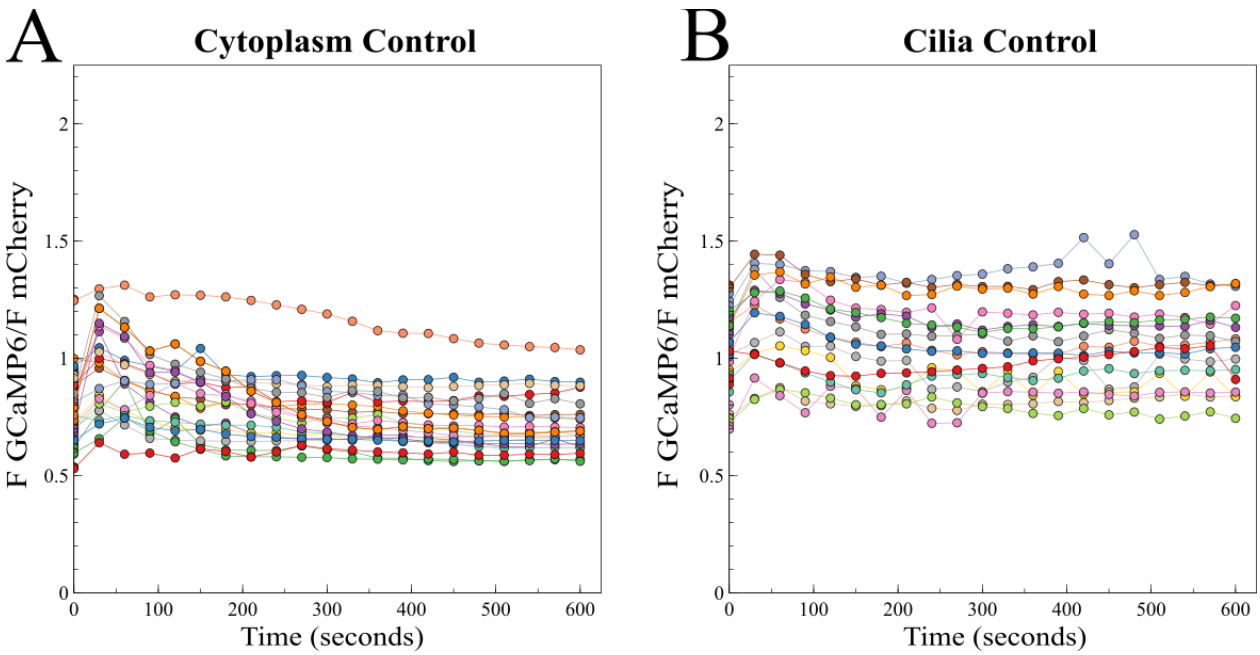

Supplemental 2. Cytoplasm and cilia single transfected control over time
Graphical representation of cytoplasm or cilia GCaMP/mCherry ratio over 600 seconds after the administration of the DMSO/water vehicle control.